HHS Public Access

Author manuscript

Sci Signal. Author manuscript; available in PMC 2016 September 20.

Published in final edited form as:

Sci Signal. ; 4(199): ra75. doi:10.1126/scisignal.2001868.

Signaling by the Matrix Proteoglycan Decorin Controls Inflammation and Cancer through PDCD4 and microRNA-21

Rosetta Merline[1], **Kristin Moreth**[1], **Janet Beckmann**[1], **Madalina V. Nastase**[1], **Jinyang Zeng-Brouwers**[1], **José Guilherme Tralhão**[2], **Patricia Lemarchand**[3], **Josef Pfeilschifter**[1], **Roland M. Schaefer**[4], **Renato V. Iozzo**[5,§], and **Liliana Schaefer**[1,§,¶]

[1]Pharmazentrum Frankfurt, Institut für Allgemeine Pharmakologie und Toxikologie, Klinikum der Goethe-Universität Frankfurt am Main, Theodor-Stern-Kai 7, 60590 Frankfurt am Main, Germany

[2]Department of Surgery, Surgery 3, Coimbra University Hospital, 3000-075 Coimbra, Portugal

[3]Inserm, UMR915, Université de Nantes, CHU de Nantes, l'Institut du thorax, 44000 Nantes, France

[4]Department of Medicine D, University Hospital of Muenster, 48149 Muenster, Germany

[5]Department of Pathology, Anatomy and Cell Biology, and the Cancer Cell Biology and Signaling Program, Kimmel Cancer Center, Thomas Jefferson University, Philadelphia, PA 19107 USA

Abstract

The mechanisms linking immune responses and inflammation with tumor development are not well understood. Here we show that the soluble form of the extracellular matrix proteoglycan decorin controls inflammation and tumor growth through PDCD4 (programmed cell death 4) and microRNA (miR) 21 by two mechanisms. First, decorin acted as an endogenous ligand of Toll-like receptor-2 and −4 and stimulated production of proinflammatory molecules, including PDCD4, in macrophages. Second, decorin prevented translational repression of PDCD4 by decreasing the

¶*Correspondence to* Liliana Schaefer, schaefer@med.uni-frankfurt.de.
§These authors made an equal contribution to the work reported in this paper.

SUPPLEMENTARY MATERIALS

Fig. S1. LPS-mediated increase in decorin abundance in macrophages in vivo and in vitro.
Fig. S2. Role of negative feedback signaling through the IL-10 receptor in the effects of decorin and LPS on TNFα and IL-12p70 protein and mRNA abundance in vivo and in vitro.
Fig. S3. Decorin treatment triggers the phosphorylation of the MAPKs p44p42 and p38 in thioglycollate-elicited macrophages in a TLR2- and TLR4-dependent manner.
Fig. S4. Analysis of decorin binding to recombinant TLR2 and to the TLR4-MD2 complex with microscale thermophoresis.
Fig. S5. Procedures to rule out contamination of decorin.
Fig. S6. Decorin- and LPS-dependent regulation of IL-10 release is mediated by miR-21 and PDCD4 in thioglycollate-elicited macrophages.
Fig. S7. Decorin-dependent regulation of *Pdcd4* expression in LPS-induced septic spleen and lungs and in Ad.DCN-transfected tumor xenografts.
Table S1. Characteristics of patients with sepsis and healthy controls.

Author Contributions: R.M. did most of the in vivo and in vitro work. K.M. performed immunoprecipitations, binding assays and was in involved in the transfection and in vivo experiments. J. B. was involved in the in vivo experiments, qPCR, transfection and immunostainings. M.V.N. was responsible for part of the Western blotting and binding assays. J.Z.B. was involved in the silencing experiments. J.G.T. and P.L. performed adenoviral expression of decorin in tumors. R.M.S. was responsible for all of the human sepsis data. R.M.S. and J.P. co-designed the study. L.S. and R.V.I. conceived and designed the study. L.S., R.M.S. and R.V.I. wrote the manuscript.

Competing Interests: The authors declare that they have no competing financial interests.

activity of transforming growth factor (TGF) β1 and the abundance of oncogenic miR-21, a translational inhibitor of PDCD4. Moreover, increased PDCD4 resulted in decreased release of the anti-inflammatory cytokine interleukin-10, thereby making the cytokine profile more proinflammatory. This pathway operates in both pathogen-mediated and sterile inflammation as shown here for sepsis and growth retardation of established tumor xenografts. In sepsis, *decorin* is an early response gene evoked by septic inflammation and decorin concentrations were increased in plasma of septic patients and mice. In cancer, decorin mediated the reduced abundance of anti-inflammatory molecules and increased that of pro-inflammatory molecules, thereby shifting the immune response to a more proinflammatory state that was associated with reduced tumor growth. Thus, by stimulating pro-inflammatory PDCD4 and decreasing the abundance of miR-21, decorin signaling boosts inflammatory activity in sepsis and suppresses tumor growth.

INTRODUCTION

Despite the mounting evidence for a relationship among innate immunity, inflammation, and tumor development (1), the mechanisms linking these processes are not well defined. PDCD4 can regulate both tumorigenesis and inflammation (2–4), and was initially identified as a protein whose abundance was increased by apoptotic stimuli and was later characterized as a tumor suppressor (2, 5). Tumor progression is associated with reduced PDCD4 synthesis (6), and therapeutic approaches that increase PDCD4 abundance inhibit neoplastic growth (11). PDCD4 can act as translational repressor of various proteins, including the anti-inflammatory cytokine interleukin-10 (IL-10) (2, 4, 12). *Pdcd4*-null mice develop spontaneous lymphomas and are less susceptible to developing inflammatory diseases (2, 4). PDCD4 abundance is controlled by multiple mechanisms (5), including phosphorylation-dependent degradation (13) and microRNA-21 (miR-21)-mediated translational repression (14, 15). Lipopolysaccharide (LPS) stimulation of Toll-like receptor (TLR) 4 results in increased abundance of miR-21, decreased PDCD4 and increased IL-10 protein (4). In contrast to PDCD4, the abundance of miR-21 has been reported to be increased in cancer cells (16), which promotes tumor growth *in vivo* (17). However, the endogenous regulation of miR-21 in inflammation and tumorigenesis is still not understood. At the posttranscriptional level, TGFβ and Smad signaling can promote the processing of primary miR-21 (pri-miR-21), resulting in increased mature miR-21 (18). In addition, TGFβ1 can increase miR-21 abundance during myofibroblast transdifferentiation in cancer stroma (19).

In addition to their structural role, the extracellular matrix (ECM) components act in their soluble forms as signaling molecules that regulate various biological processes, including inflammation, tumor growth and metastasis (20, 21). Cross-talk between cancer cells and the tumor microenvironment regulate the amounts of inflammatory cytokines, which are key modulators of tumor growth (1, 22). Some ECM molecules are endogenous ligands of Toll-like receptors (TLRs), which function in innate immune responses (23). ECM components are normally sequestered and are therefore not recognized by the immune system, but when released under tissue stress, they may act as damage-associated molecular patterns (DAMPs), triggering sterile inflammation and potentiating pathogen-mediated inflammation (23, 24).

Decorin, a small leucine-rich proteoglycan of the ECM can serve as a ligand for receptor tyrosine kinases, including EGFR, IGF-IR, and Met (10). Decorin is an endogenous inhibitor of TGFβ1 (25, 26), and inhibits primary tumor growth and metastatic spreading by decreasing the activity of EGFR and Met and by reversing TGFβ-induced immunosuppression (9). Evidence has suggested a role for decorin in various inflammatory processes, such as in the synthesis of monocyte chemotactic protein-1 (MCP-1) involved in the recruitment of monocytes to the site of injury (27), inhibition of macrophage proliferation and apoptosis (28), and counteracting the repressive effects of TGFβ on macrophage activation (29).

In this study, we identified a role of decorin in inducing the proinflammatory tumor suppressor PDCD4 by driving synthesis of PDCD4 in a TLR2- and TLR4-dependent pathway and by attenuating TGFβ1- and miR-21-mediated inhibition of PDCD4. We showed that soluble decorin is an endogenous ligand of TLR2 and TLR4 and provided detailed mechanistic insights into decorin-dependent proinflammatory signaling down-stream of TLR2, TLR4, and PDCD4. This pathway appears to operate in two different types of inflammation, pathogen-mediated inflammation in the context of sepsis and sterile inflammation in the context of established tumor xenografts. Our findings might be particularly relevant for the treatment of neoplastic diseases, and the ability of decorin to decrease the abundance of miR-21, immunosuppressive TGFβ1, and anti-inflammatory IL-10 as well as to stimulate the production of proinflammatory PDCD4, TNFα, and IL-12 suggests that decorin might represent an attractive target for cancer therapy.

RESULTS

Decorin abundance is increased in septic patients and in mice with LPS-induced sepsis

Decorin modulates the activity of growth factors that might be involved in regulating the immune system (25, 26, 28, 29). We therefore measured circulating decorin in plasma samples from a cohort of male and female patients with sepsis ranging in age from 24–78 years and suffering from Gram-negative or -positive infections (table S1). Immunoblot analysis and ELISA revealed increased amounts of decorin protein core in septic patients as compared to healthy individuals ($P < 0.01$) (Fig. 1, A and B). These results suggest that decorin may be part of the inflammatory response and that its abundance is enhanced by systemic inflammation independently of age, sex or the causative organism.

To study the regulation of decorin in inflammation-associated immune responses, we experimentally induced sepsis with LPS in $Dcn^{+/+}$ and $Dcn^{-/-}$ mice and found that plasma concentrations of decorin were enhanced in septic $Dcn^{+/+}$ mice as detected by immunoblotting (Fig. 1C) and ELISA (Fig. 1D). Also, *Dcn* mRNA and protein abundance in the lung was increased (Fig. 1E and F). Immunohistochemical staining showed enhanced decorin accumulation in septic $Dcn^{+/+}$ lungs mainly in the perivascular space (Fig. 1G) and in the vicinity of macrophages (fig. S1A). Partial apical cytoplasmic and membranous positivity for decorin was observed in bronchial epithelial cells (Fig. 1H). Lungs from septic $Dcn^{-/-}$ mice served as controls for specificity of the staining (Fig. 1, G and H). The localization of decorin in close proximity to macrophages in LPS-induced septic lungs (fig. S1A) prompted us to investigate whether LPS stimulates macrophages to synthesize decorin.

Peritoneal macrophages showed enhanced *Dcn* mRNA expression as early as 30 min after LPS stimulation (fig. S1B) as well as increased secretion of decorin (fig. S1C).

Thus, analogous to septic human patients, mice show increased circulating decorin shortly after the induction of sepsis. These findings, together with enhanced decorin mRNA and protein abundance in septic lungs and in LPS-stimulated macrophages, suggest that *Dcn* is an early response gene that is transcriptionally activated by septic inflammation.

Decorin deficiency attenuates the proinflammatory effects of LPS

Next, we induced sepsis with a sublethal dose of LPS in $Dcn^{+/+}$ and $Dcn^{-/-}$ mice and monitored the temporal changes in the abundance of several cytokines. In septic $Dcn^{-/-}$ compared to $Dcn^{+/+}$ mice, the plasma concentration of the anti-inflammatory cytokine IL-10 was increased (Fig. 2A) and those of the proinflammatory cytokines TNFα (Fig. 2B) and IL-12p70 (Fig. 2C) were decreased. After a lethal dose of LPS, IL-10 abundance was higher in the spleens and lungs of septic $Dcn^{-/-}$ mice than in those of septic $Dcn^{+/+}$ mice (Fig. 2, D and E). *Il10* mRNA expression in the lungs (Fig. 2F) of septic mice did not correlate with the amount of protein, suggesting that decorin could inhibit LPS-mediated induction of IL-10 at the translational level.

Analysis of proinflammatory cytokines revealed decreased TNFα protein abundance in spleen and lungs (Fig. 2, G and H) and reduced pulmonary *Tnf* expression (Fig. 2I) in septic $Dcn^{-/-}$ mice. Furthermore, septic $Dcn^{-/-}$ mice had lower amounts of splenic and pulmonary IL-12p70 protein (Fig. 2, J and K) and decreased pulmonary *Il12b* expression (Fig. 2L). Thus, decorin deficiency attenuated the sepsis-induced increase in the amounts of TNFα and IL-12p70 while increasing IL-10 concentrations in target organs and in plasma, suggesting a role for decorin as a differential regulator of pro- and anti-inflammatory cytokines in LPS-induced sepsis.

Exogenous decorin reverses the development of the inflammatory cytokine profile in septic $Dcn^{-/-}$ mice

To provide direct in vivo evidence for decorin-mediated regulation of LPS signaling, $Dcn^{-/-}$ mice were injected with recombinant human decorin followed by intraperitoneal injection of LPS. Decorin-injected mice showed reduced plasma concentrations of IL-10 (Fig. 3A) and increased plasma concentrations of TNFα and IL-12p70 (Fig. 3, B and C) compared to untreated septic $Dcn^{-/-}$ mice. Decorin-treated septic $Dcn^{-/-}$ mice showed decreased IL-10 protein abundance in the spleen and lungs (Fig. 3, D and E) but higher levels of *Il10* mRNA in the lungs (Fig. 3F). Furthermore, they showed increased amounts of the proinflammatory cytokine TNFα (Fig. 3, G and H) in the spleen and lungs and increased levels of *Tnf* in lungs (Fig. 3I). Similar results were obtained for IL-12p70 protein abundance (Fig. 3, J and K) and *Il12b* expression (Fig. 3L). These results reinforce the notion that soluble decorin enhances the production of proinflammatory cytokines in LPS-induced sepsis, while suppressing LPS-mediated increases in IL-10 concentrations by inhibiting *Il10* translation.

$Dcn^{-/-}$ mice injected with decorin in the absence of LPS showed enhanced concentrations of TNFα and IL-12p70 in plasma (Fig. 3, B and C), spleen (Fig. 3, G and J), and lungs (Fig. 3, H and K). Corresponding increases in the expression of *Tnf* (Fig. 3I) and *Il12b* (Fig. 3L)

were detected in the lungs. Furthermore, administration of decorin in the absence of LPS resulted in increased IL-10 protein in plasma (Fig. 3A), spleen (Fig. 3D), and lungs (Fig. 3E) with a minor increase in *Il10* mRNA expression in the lungs (Fig. 3F). Thus, administration of soluble decorin in mice can mimic the effects of LPS by increasing the concentrations of the proinflammatory molecules TNFα and IL-12p70 and that of the anti-inflammatory cytokine IL-10. By contrast, decorin when combined with LPS inhibits LPS-mediated increases in IL-10 synthesis in vivo at the translational level. Therefore, it is possible that, in the presence of LPS, the increase in TNFα and IL-12p70 production may be caused not only by the direct effects of decorin, but also by reduced negative feedback signaling through the IL-10 receptor (30). To address this issue, LPS-induced sepsis with or without administration of exogenous decorin was induced in $Il10^{-/-}$ and C57BL/6 mice. As expected, in septic mice IL-10 deficiency enhanced the amount of TNFα and IL-12p70 in plasma (fig. S2, A and B), spleen (fig. S2, C and D), and lungs (fig. S2, E and F) and increased the mRNA abundance of *Tnf* (fig. S2G) and *Il12b* (fig. S2H) in lungs. Moreover, administration of exogenous decorin further increased the amounts of TNFα (fig. S2 A, C, E) and IL-12p70 (fig. S2, B, D, F) protein as well as their respective mRNAs (fig. S2, G and H) both in septic $Il10^{-/-}$ and C57BL/6 mice. Thus, these data indicate that decorin-mediated enhancement of TNFα and IL-12 after LPS stimulation is a combined effect of (i) decorin-mediated direct induction of TNFα and IL-12 synthesis and (ii) reduced negative feedback signaling through the IL-10 receptor.

Decorin induces TNFα and IL-12p70 release from macrophages through TLR2 and TLR4

To explain the decorin-induced synthesis of TNFα and IL-12 in septic and healthy mice, we investigated the effects of decorin on the synthesis of these cytokines in peritoneal macrophages. Decorin stimulation increased the release of TNFα from $Dcn^{+/+}$ macrophages in a dose- and time-dependent manner (Fig. 4A), whereas IL-12p70 release was stimulated in a dose-dependent manner at 6 hours, with a decrease at 24 hours (Fig. 4B). Macrophages incubated over 6 hours with decorin exhibited increased mRNA abundance of both *Tnf* and *Il12b* (Fig. 4, C and D). Moreover, co-stimulation of macrophages with LPS and decorin resulted in enhanced secretion of TNFα and IL-12p70 compared to LPS stimulation alone (Fig. 4, E and F).

We have previously shown that the small leucine-rich proteoglycan biglycan induces TNFα release from macrophages by signaling through the innate immunity receptors TLR2 and TLR4 (7). Similar to biglycan, decorin activated the MAPKs p44p42 and p38 (fig. S3) in macrophages and increased the release of TNFα (Fig. 4G) and IL-12p70 (Fig. 4H) in a TLR2- and TLR4-dependent manner.. Binding assays in HEK cells stably expressing TLR2 or TLR4 indicated that decorin could pull-down TLR2 and TLR4 (Fig. 4, I and J). We also used microscale thermophoresis to analyze and confirm the binding of fluorescence-labeled human decorin to recombinant human TLR2 (fig. S4A) and to the TLR4-MD2 MD2 complex (MD2 also known as lymphocyte antigen 96 is an adaptor molecule for TLR4) (31) (fig. S4B). Decorin bound to TLR2 with a Kd of 59 ± 10 nM (fig. S4A) and to the TLR4-MD2 complex with a Kd of 37 ± 5 nM (fig. S4B). Ligand binding and activation of TLR2 and TLR4 leads to the nuclear translocation and activation of the transcription factor NF-κB (nuclear factor κB) (32), Following binding, the ability of decorin to activate TLR2 and

TLR4 was analyzed with a reporter gene assay that coupled NF-κB transcriptional activation to the activity of secreted alkaline phosphatase (SEAP). Stimulation with decorin led to activation of NF-κB as indicated by increased SEAP activity in HEK-Blue-hTLR2 (Fig. 4K) and HEK-Blue-hTLR4 cells (Fig. 4L). Together these results demonstrate that soluble decorin autonomously triggers the production of TNFα and IL-12p70 in macrophages through TLR2 and TLR4. In the presence of LPS decorin enhances the effects of LPS by also signaling through TLR2.

To ensure that activation of macrophages by decorin was not attributable to contamination of the decorin preparation, we ruled out the presence of LPS, various proinflammatory factors, and other TLR4 and TLR2 ligands (fig. S5, A–G). Endotoxin contamination of 8 μg/ml decorin corresponded to 16 pg/ml of LPS. Release of TNFα (fig. S5A) or IL-12p70 (fig. S5B) was stimulated by decorin, but not by LPS. Boiling decorin but not LPS abolished the increased release of TNFα (fig. S5C) or IL-12p70 (fig. S5D) from macrophages. Preincubating macrophages with polymyxin B inhibited LPS- but not decorin-mediated release of TNFα (fig. S5E) and IL-12p70 (fig. S5F). Furthermore, decorin or LPS but not peptidoglycan activated the NF-κB reporter gene in HEK-Blue-hTLR4 cells (fig. S5G). Preincubation with polymyxin B abolished LPS- but not decorin-mediated activation of the NF-κB reporter gene in HEK-Blue-hTLR4 cells (fig. S5G). The purity of intact and chondroitinase ABC-digested decorin was demonstrated by silver staining (fig. S5H). Finally, only intact decorin, not the protein core or the glycosaminoglycan (GAG) chain of decorin (obtained by β-elimination), could trigger macrophage release of TNFα (fig. S5I) or IL-12p70 (fig. S5J), indicating these effects were not caused by contaminants, such as LPS, TLR ligands, other proinflammatory factors or glycosaminoglycan (GAG) chains.

Decorin increases PDCD4 abundance and inhibits LPS-mediated IL-10 production in macrophages

Because PDCD4 is a translational repressor of IL-10 (2), we wanted to investigate whether decorin could regulate PDCD4. Stimulation of wild-type macrophages with decorin led to increased abundance of PDCD4 protein (Fig. 5A). PDCD4 abundance is increased by LPS-stimulation of TLR4 (4), and indeed, the decorin-mediated increase in PDCD4 abundance in response to LPS was reduced in TLR4 (and TLR2) deficient macrophages and abolished in macrophages deficient for both receptors (Fig. 5A). In LPS-treated RAW264.7 and bone marrow-derived mouse macrophages, PDCD4 protein synthesis is controlled by multiple mechanisms resulting in an initial increase in PDCD4 abundance (1–4 hours after LPS treatment) followed by a substantial decrease in PDCD4 protein within 8 hours after LPS stimulation (4). Consistent with these results, stimulation of peritoneal macrophages for 8 hours with either decorin or LPS resulted in reduced PDCD4 abundance (Fig. 5, B and C). However, the decline in PDCD4 abundance was less pronounced in macrophages stimulated with decorin compared to LPS-treated cells (Fig. 5, B and C).

miR-21 plays a crucial role in LPS-induced reduction of PDCD4 abundance (4). We found that stimulating macrophages with decorin or LPS for 8 hours increased miR-21 abundance (Fig. 5D). Thus, similar to LPS, decorin enhances PDCD4 abundance at early time points (2 hours) (Fig. 5A), whereas at later times (8 hours) LPS and decorin both increase miR-21

expression, which might have suppressed PDCD4 protein abundance (Fig. 5, B–D). Co-stimulation of LPS-treated macrophages with decorin reduced the expression of miR-21 (Fig. 5D), suggesting that decorin-mediated inhibition of LPS-induced synthesis of IL-10 might occur at the level of miR-21 regulation.

To provide further evidence that LPS- or decorin-dependent effects on IL-10 were mediated by miR-21 and PDCD4, we performed in vitro silencing experiments. Transient transfection of wild-type macrophages with antisense oligonucleotides specific for miR-21 attenuated the increase in miR-21 expression induced by decorin or LPS (fig. S6A), which was associated with increased PDCD4 abundance at 8 hours (fig. S6B) and lower concentrations of IL-10 in culture media at 24 hours (fig. S6C). To further prove that the reduction in IL-10 concentration was mediated by PDCD4, macrophages were transfected with small interfering RNA (siRNA) specific for PDCD4 (100 nM). Transfection with PDCD4 siRNA, as opposed to control siRNA, resulted in decreased PDCD4 abundance in macrophages stimulated either with LPS or decorin alone or with a combination of both (fig. S6, D and E) and resulted in increased IL-10 release from macrophages stimulated either with LPS or decorin or both (fig. S6F). Thus, these results show that miR-21 and PDCD4 are important mediators of LPS- and decorin-dependent regulation of IL-10 production in macrophages.

TGFβ1 stimulates miR-21 biogenesis in fibroblasts (19) and miR-21 processing in smooth muscle cells (18). Decorin, on the other hand, is an endogenous inhibitor of TGFβ1 (25, 26), and in macrophages, reverses the repressive effects of TGFβ1 on cell activation (29). We therefore hypothesized that the suppressive effects of decorin on LPS-stimulated increases in miR-21 expression might be due to inhibition of TGFβ1. We found that LPS but not decorin stimulated the secretion of active TGFβ1 in macrophages (Fig. 5E), and co-stimulation of macrophages with both LPS and decorin substantially reduced the amounts of active TGFβ1 (Fig. 5E).

We incubated LPS- or decorin-stimulated macrophages with a TGFβ1 neutralizing antibody, which increased PDCD4 abundance in macrophages treated with LPS (Fig. 5, B and C). These effects could be mimicked by addition of decorin to LPS-stimulated macrophages (Fig. 5, B and C). In agreement with our observation that decorin, in contrast to LPS, does not induce TGFβ1 release in macrophages (Fig. 5E), we found that the TGFβ1 neutralizing antibody did not affect PDCD4 abundance in decorin-treated macrophages (Fig. 5, B and C). Furthermore, when added to LPS-stimulated macrophages, the TGFβ1 neutralizing antibody decreased miR-21 expression (Fig. 5D). Taken together, these findings demonstrate that decorin and TGFβ1 neutralization repress the expression miR-21. Consistently, macrophages costimulated with LPS and exogenous TGFβ1 showed increased miR-21 expression compared to cells stimulated with only LPS, an effect that was reversed either by addition of decorin or the TGFβ1 neutralizing antibody (Fig. 5D).

Finally, we addressed the issue whether these mechanisms were involved in decorin-mediated inhibition of LPS-induced release of IL-10. As expected, decorin or LPS alone enhanced IL-10 release after 24 hours (Fig. 5F). However, macrophages costimulated with decorin and LPS secreted lower amounts of IL-10 compared to those stimulated with LPS alone (Fig. 5F). Thus, the in vitro data reflect the in vivo observations in plasma and tissue

samples from septic mice (Fig. 3A, D, E). The inhibitory effects of decorin on LPS-stimulated secretion of IL-10 were mimicked by adding the TGFβ1 neutralizing antibody (Fig. 5F). Conversely, co-stimulation of macrophages with LPS and exogenous TGFβ1 further enhanced the amounts of secreted IL-10 (Fig. 5F). These effects were attenuated either by decorin or TGFβ1 neutralizing antibody (Fig. 5F). Thus, the pattern of IL-10 abundance (Fig. 5F) reflected the expression profile of miR-21 (Fig. 5D).

Furthermore, when stimulated with LPS, *Il10*$^{-/-}$ macrophages with LPS released more TNFα (fig. S2I) and IL-12p70 (fig. S2J) than C57BL/6 macrophages. However, addition of decorin to *Il10*$^{-/-}$ or C57BL/6 macrophages stimulated with LPS further increased secretion of TNFα (fig. S2I) and IL-12p70 (fig. S2J), indicating that this enhancement was partially mediated by decorin and not only caused by reduced negative feedback signaling through the IL-10 receptor.

Taken together, our data demonstrate that decorin increases PDCD4 abundance with subsequent inhibition of LPS-mediated IL-10 release by two mechanisms: i) by increasing PDCD4 abundance in a TLR2- and TLR4-dependent manner and ii) by inhibiting the TGFβ1-induced increase in miR-21 expression, a posttranscriptional suppressor of PDCD4.

Absence of decorin prevents increase in PDCD4 abundance and enhances expression of miR-21 and abundance of active TGFβ1 in LPS-induced septic mice

Next, we determined the amounts of PDCD4, miR-21, and active TGFβ1 in tissue samples of septic mice. In septic spleen and lungs, *Dcn*$^{-/-}$ mice had lower protein (Fig. 6, A–D) and mRNA (fig. S7, A and B) abundance of PDCD4 compared to *Dcn*$^{+/+}$ mice after injection of a lethal dose of LPS. This phenotype was rescued by systemic administration of decorin (Fig. 6, A–D and fig. S7, A and B). Furthermore, septic *Dcn*$^{-/-}$ mice had increased miR-21 expression in spleen and lungs compared to septic *Dcn*$^{+/+}$ mice, effects that were reversed by systemic administration of exogenous decorin in *Dcn*$^{-/-}$ mice (Fig. 6, E and F). Moreover, septic *Dcn*$^{-/-}$ mice had higher amounts of active TGFβ1 in the spleen and lungs compared to *Dcn*$^{+/+}$ mice, a phenotype that was attenuated by exogenous decorin in septic *Dcn*$^{-/-}$ mice (Fig. 6, G and H).

Thus, in *Dcn*$^{-/-}$ septic mice and *Dcn*$^{-/-}$ septic mice treated with decorin the amount of IL-10 (Fig. 2, D and E) inversely correlated with that of PDCD4 (Fig. 6, A–D) and positively correlated with that of active TGFβ1 (Fig. 6, G and H) or miR-21 (Fig. 6, E and F). These data from septic mice corroborate our in vitro results in macrophages. The enhanced miR-21 expression and active TGFβ1 concentration in the septic spleen and lungs in the absence of decorin in vivo can explain the reduced PDCD4 abundance observed under these conditions. We suggest a paradigm in which decorin reduces the abundance of miR-21 by binding and inhibiting TGFβ1 induced by LPS, leading to increased PDCD4 abundance and subsequent suppression of IL-10 translation.

Decorin overexpression in tumor xenografts induces a proinflammatory immune response through miR-21 and PDCD4

We further speculated that the ability of decorin to increase PDCD4 abundance, promote proinflammatory responses in macrophages, and inhibit TGFβ1-mediated miR-21

maturation and IL-10 synthesis could retard tumor growth. In agreement with the data from septic mice and macrophages, established tumor xenografts injected with a vector containing exogenous full-length decorin cDNA Ad.DCN had decreased IL-10 (Fig. 7A) abundance, increased TNFα and IL-12p70 abundance (Fig. 7, B and C), and increased *Il10* expression (Fig. 7D) compared to those injected with the control adenovirus (Ad.null). The expression of *Tnf* and *Il12b* mRNAs (Fig. 7, E and F) was enhanced in the Ad.DCN-injected tumor xenografts. *Pdcd4* expression and PDCD4 abundance was increased in xenografts injected with Ad.DCN compared to Ad.null tumors, as analyzed by qPCR (fig. S7C), immunoblotting (Fig. 7, G and H), and immunostaining (Fig. 7I). Analysis of tumor xenografts injected with Ad.DCN showed increased amounts of cleaved caspase-3, a downstream mediator of PDCD4 (Fig. 7, G and J), further confirming the ability of decorin to increase PDCD4 abundance and suggesting that the antitumoral effects of decorin were mediated by enhanced apoptosis (33, 34). Increased decorin abundance in the xenografts also led to decreased amounts of active TGFβ1 (Fig. 7K) and lower expression of miR-21 (Fig. 7L). We previously reported that Ad.DCN injection suppressed tumor growth (33). Here we show an association between the reduced volume of Ad.DCN-injected tumors and decreased amounts of IL-10 (Fig. 7M) as well as enhanced concentrations of TNFα (Fig. 7N) and IL-12p70 (Fig. 7O) in individual tumors. Multiple regression analysis with two independent predictor variables (volume of Ad.DCN and Ad.null tumors) and one criterion variable were statistically significant for TNFα, IL-12p70, and IL-10, confirming the link between inceased decorin abundance, enhanced inflammatory immune response, and reduced tumor volumes.

In summary, these data provide evidence for a mechanism of decorin-mediated inhibition of tumor growth. Decorin decreased the expression of the oncogene miR-21, increased the abundance of the tumor suppressor PDCD4, and shifted the immune response to a proinflammatory axis, which was associated with growth retardation of established tumors.

DISCUSSION

In this report we show that the soluble ECM component decorin gives rise to proinflammatory signaling. We have identified decorin as an enhancer of PDCD4 abundance, a tumor suppressor, mediated by its ability to bind and inhibit active TGFβ1-mediated increase of oncogenic miR-21, a translational inhibitor of PDCD4. Furthermore, we show that decorin is a ligand of TLR2 and TLR4 and stimulates the production of proinflammatory PDCD4, TNFα, and IL-12 in macrophages. Increased PDCD4 triggers a decrease in the production of the anti-inflammatory cytokine IL-10, thereby further driving the cytokine profile towards a proinflammatory phenotype. These mechanisms are relevant in vivo in the context of innate immunity and tumor growth retardation. With regards to innate immune responses, we show that patients with Gram-positive or -negative sepsis had increased plasma concentrations of circulating decorin. In experimental sepsis, we identified *Dcn* as an early response gene triggered by LPS. It is conceivable that soluble decorin enhances the stimulatory effects of LPS on the abundance of PDCD4, TNFα, and IL-12p70 through TLR2. In established tumors, exogenously administered decorin acts as DAMP and exerts its proinflammatory effects through TLR2 and TLR4. In sepsis and cancer decorin additionally increases PDCD4 abundance by preventing its posttranscriptional suppression

independently of TLR2 or TLR4 by inhibiting TGFβ1 signaling and decreasing miR-21 expression. A working model summarizing this concept is shown in Fig. 8.

Enhanced concentration of circulating decorin in the plasma of patients with sepsis caused by either Gram-negative or -positive bacteria suggested a role for this proteoglycan in acute inflammation. We used a model of LPS-mediated systemic inflammation in $Dcn^{+/+}$ and $Dcn^{-/-}$ mice and determined by two independent methods that circulating decorin increased rapidly in septic $Dcn^{+/+}$ mice. Therefore, we felt confident that the LPS-induced sepsis was an appropriate model for analyzing the effects of soluble decorin in systemic inflammation. Furthermore, *Dcn* expression and decorin abundance were increased in lungs from $Dcn^{+/+}$ septic mice, indicating that the rise of plasma decorin in sepsis was most likely due to de novo synthesis of this proteoglycan in target organs. This is in agreement with a previous report showing that IL-6 and IL-10 induced an increase in *Dcn* expression in pulmonary endothelial cells (35). Enhanced decorin accumulation localized in close proximity to infiltrating macrophages suggested that macrophages might be one of the sources of de novo decorin synthesis. In fact, macrophages exposed to LPS rapidly showed increased *Dcn* mRNA abundance and secreted the proteoglycan into the culture medium. These findings, together with the detection of the intact protein core in plasma, suggests that *Dcn* is an early response gene in sepsis. It cannot be excluded that proteases secreted by infiltrating or resident pulmonary cells might also liberate sequestered decorin from the ECM, thereby swiftly increasing its concentration in the circulation.

Septic *Dcn*-null mice had lower plasma and tissue concentrations of the proinflammatory cytokines TNFα and IL-12p70 with correspondingly lower tissue expression of the respective mRNAs, effects that were reversed by exogenous administration of recombinant human decorin. In healthy $Dcn^{-/-}$ mice administration of exogenous decorin triggered expression of *Tnf* and *Il12b* mRNAs and increased TNF-α and IL-12p70 abundance in the spleen and lungs resulting in enhanced concentrations of both cytokines in plasma. These *in vivo* data suggest that decorin by itself can mimic the effects of LPS. This is further confirmed by our *in vitro* findings that soluble decorin is an endogenous ligand of TLR2 and TLR4 as supported by the mechanistic data generated in macrophages and HEK cells overexpressing TLR2 or TLR4 as well as in binding studies.

Like decorin, the small leucine-rich proteoglycan biglycan also signals through both TLR2 and TLR4 (7), thereby regulating pathogen-mediated and sterile inflammation (7, 36) and mediating both innate and adaptive immune responses (37). Similar to biglycan (7), only intact decorin, but not the protein core or GAG chain of decorin, increased the release of TNFα and IL-12p70 from macrophages. Therefore, decorin-dependent stimulation of macrophages is not due to a general effect of GAG chains, which is involved in the activation of chemokines (38), but is in fact specific for the intact decorin. Taking into account the complexity of TLR2 and TLR4 signaling, which requires various adaptor molecules (39), it is conceivable that several binding sites of decorin both on the protein core and within the GAG chain might be important for TLR2 and TLR4 activation. The second proinflammatory effect of decorin signaling occurs because of attenuation of TGFβ1 activity. Binding of decorin to TGFβ1 involves the Leu^{155}-Val^{260} domain of the decorin protein core (40), whereas the GAG chain prevents this interaction (41). Several studies

indicate that decorin neutralizes the effects of TGFβ1 by interfering with TGFβ1 signaling, rather than physically interacting with TGFβ1 (42). The role of decorin GAGs in inhibition of TGFβ1 signaling remains to be determined. Therefore, a role of the GAG chain in the regulation of the TGFβ1, miR-21, PDCD4 and IL-10 axis cannot be excluded. Decorin acts as a signaling molecule and ligand to several receptor tyrosine kinases, such as the EGFR, Met, and IGF-IR (10).

A key finding of our study is the observation that decorin increases PDCD4 abundance. Exogenous decorin had differential in vivo effects on the translational regulation of IL-10 depending on whether decorin was administered alone or together with LPS. Decorin alone increases *Il10* expression and IL-10 abundance, whereas in combination with LPS decorin further boosts the LPS-mediated increase in of *Il10* expression but suppresses the LPS-triggered increase in IL-10 abundance. These results could be explained by our findings that soluble decorin signals through TLR2 and TLR4 thereby inducing *Il10* expression and enhancing PDCD4 abundance, which suppresses translation of IL-10 and hence its protein abundance. However, as it has been reported that IL-10 inhibits TNFα (43) and IL-12 (44) protein abundance. Therefore it cannot be ruled out that the increased in vitro and in vivo production of TNFα and IL-12 cytokines caused by addition of decorin to LPS might have been partially affected by dampened feedback signaling through the IL-10 receptor. In fact, data from septic $Il10^{-/-}$ mice and $Il10^{-/-}$ macrophages indicate that decorin-mediated enhancement of the effect of LPS on TNFα and IL-12 production is a combined effect of decorin-mediated direct induction of TNFα and IL-12 production and reduced negative feedback signaling through the IL-10 receptor.

The initial LPS-mediated increase in PDCD4 abundance is followed by a substantial decline (4), caused by the LPS-induced increase in miR-21 abundance, which targets *Pdcd4* mRNA (14, 45), and a subsequent induction of IL-10 production Accordingly, we found that PDCD4 abundance in macrophages declined after 8 hours of incubation with decorin or LPS. It is conceivable that decorin stimulates miR-21 transcription as a ligand to TLR4 and TLR2. Therefore, augmentation of LPS mediated effects on miR-21 expression was expected in the presence of decorin, similar to the pattern obtained for TNFα and IL-12. We showed that LPS- or decorin-dependent effects on IL-10 abundance were mediated by miR-21 and PDCD4 in thioglycollate-elicited macrophages, and that addition of decorin attenuated the ability of LPS to increase the abundance of miR-21 and PDCD4 and decrease IL-10 abundance both in vivo and in vitro. These observations indicate that decorin is capable of suppressing miR-21 expression through an additional mechanism, which is apparently more potent than decorin-, TLR2-, and TLR4-dependent induction of miR-21.

TGFβ1 signaling can increase the amount of mature miR-21 by promoting the processing of primary miR-21 into precursor miR-21 (18). Decorin is an endogenous inhibitor of TGFβ1 that interferes directly and indirectly with the TGFβ1 signaling cascade (25, 26, 41, 46). Furthermore, LPS but not decorin increases the release of active TGFβ1 in vivo and in vitro (47, 48). Thus, inhibition of TGFβ1 signaling by decorin might be the missing link that explains how decorin suppresses the LPS-stimulated increase in miR-21 expression. Accordingly, we found that miR-21 expression was increased by exogenous TGFβ1 and decreased by a neutralizing TGFβ1 antibody, and the latter effect was mimicked by

administration of decorin. These results might help to explain the mechanism by which decorin reverses TGFβ-mediated immunosuppression in macrophages and tumors (29, 49). Together, our data suggest that decorin increases PDCD4 abundance by inducing PDCD4 synthesis through TLR2 and TLR4 and by inhibiting the TGFβ1- and miR-21-mediated suppression of PDCD4 translation.

In a tumor xenograft model, adenoviral transfection with decorin resulted in increased *Pdcd4* expression and PDCD4 abundance, decreased miR-21 abundance, and a shift of the immune response towards a proinflammatory phenotype in established tumors. Our data are consistent with the observation that tumor proliferation and invasion are both associated with increased expression of miR-21 (17), which promotes tumor growth (17) and with decreased abundance of PDCD4 (5, 14), which is antitumorigenic (2, 3). Furthermore, experimental strategies that increase IL-12 abundance (50, 51) or decrease IL-10 (52) or TGFβ1 (53) abundance result in tumor growth retardation. In contrast, reduced tissue decorin abundance correlates with a poor prognosis in invasive breast cancer (54), in aggressive soft tissue tumors (55), and during mammary gland carcinogenesis in Tientsin Albino 2 TA2 mice with spontaneous breast cancer (56). Decorin-mediated inhibition of tumor growth has been previously correlated with enhanced apoptosis in a tumor xenograft model (33). Here we show that increased abundance of decorin leads to an increase in active caspase-3, a downstream effector of PDCD4 (57), which suggests an additional link between decorin-induced growth inhibition and apoptosis. Higher amounts of active caspase-3 have also been detected in an orthotopic xenograft model (20, 34) following systemic delivery of decorin protein core.

Multifunctional involvement of proteoglycans makes them both potential targets for cancer remedies as well as novel antitumoral therapeutic agents (58, 59). Small leucine-rich proteoglycans, such as decorin and lumican, act as tumor repressors (58). Local or systemic delivery of recombinant decorin exerts antioncogenic effects, which are attributed to the ability of decorin to bind to and decrease the abundance of several receptor tyrosine kinases (9). In orthotopic xenograft models of squamous cell carcinoma (34) and mammary carcinoma (20), administration of the decorin protein core reduces tumor growth, induces apoptosis in a dose-dependent manner and prevents lung metastasis. These effects are achieved through the binding of decorin with EGFR on tumor cells with high EGFR abundance, an interaction that leads to decreased surface abundance of EGFR (9, 10). In addition, decorin administration reduces tumor size by interacting with and decreasing the surface abundance of EGFR and Met (60) in an orthotopic model of prostate cancer (61). In addition, decorin also causes degradation of β-catenin and Myc, which are downstream effectors of Met (62). In fact, systemic administration of decorin results in decreased surface abundance of Met followed by suppression of β-catenin and Myc in various tumor xenograft models (62). Here, we demonstrate that the decorin-mediated reduction of tumor volume is associated with decreased IL-10 abundance and increased concentrations of TNFα and IL-12p70 in individual tumors. Thus, our findings shed new light on the tumoricidal effects of decorin, which are based on a TLR2-, TLR4-, and PDCD4-mediated proinflammatory immune response. These findings may lead to novel therapeutic strategies for the treatment of malignant disorders. Thus, targeting matrix-derived signaling might lead to the development of more selective drugs for the treatment of sepsis and cancer.

MATERIALS AND METHODS

Patients with sepsis and healthy controls

Patients admitted in the Intensive Care Unit of the Department of Medicine D, University Hospital, University of Muenster from January 01 to July 31, 2009 were enrolled in this study. All patients presented clinical and laboratory findings that fulfilled the criteria for sepsis, as defined by the American College of Chest Physicians and Society of Critical Care Medicine Consensus Conference Committee (63). The study was approved by institutional review board of the Medical Faculty, University of Muenster and written informed consent was obtained from patients and volunteers. Severity of disease was evaluated using the Acute Physiology and Chronic Health Evaluation (APACHE II) classification system (64). A total of 15 patients were enrolled having an APACHE II score of 27.8 ± 0.60. The mean age (± SEM) was 54 ± 4 years (age range: 24–78 years), and the female to male ratio was 7 to 8. The control group consisted of 10 healthy volunteers, with an average age of 52 ± 6 years (age range: 23–81 years), and a male to female ratio of 1 to 1.

Animals and induction of sepsis

All animal experiments were conducted in accordance with the German Animal Protection Act and were approved by the Ethics Review Committee for laboratory animals of the District Government of Muenster and Darmstadt, Germany. The *Dcn*$^{+/+}$, and *Dcn*$^{-/-}$, *Tlr2*$^{-/-}$, *Tlr4*$^{-/-}$, *Tlr2*$^{-/-}$ and *Tlr4-M* mice were previously described (7, 65). *Il10*$^{-/-}$ (C57BL/6 background) mice were purchased from The Jackson Laboratory and C57BL/6 and C3H/HeN mice from Charles River Laboratories. Sepsis was induced in 8-week-old mice by intraperitoneal (i.p.) injection of 50 mg/kg (for a lethal dose) or 10 mg/kg (for a sublethal dose) of LPS (*Salmonella minnesota*, Sigma or ultra-pure, Invivogen). Recombinant human decorin (65), 5 mg/kg per mouse reconstituted in physiological saline was administered intravenously. Animals were sacrificed at the end of the experiment (2 hours or as indicated) and the plasma and organs were processed for further analysis.

Induction of A549 tumor xenografts and in vivo decorin gene transfer

Four-week-old female *nu/nu* mice (Janvier) were purchased from Charles River Laboratories and A549 tumor xenografts were established in the subcutaneous space as described previously (33). When the tumor reached a volume of 50–150 mm^3, animals received an intratumoral injection of Ad.DCN (vector containing exogenous full-length decorin cDNA) or control vector Ad.null (vector containing no exogenous gene) (5×10^9 plaque-forming units per injection) at days 0, 3, and 6. Animals were sacrificed at the end of the experiment (10 days after the first vector injection). Tumors were dissected and processed for further analysis. Tumor volume was calculated as $axb^2/2$, where a = larger diameter and b = smaller diameter (33).

Isolation of decorin from septic plasma, SDS-PAGE, Western blotting and ELISA

Decorin in the plasma from humans and mice (200 μl) was extracted, semipurified and digested with chondroitinase ABC (Seikagaku Corporation) as described previously (7, 37). Processing of tissue homogenates and cell lysates, SDS-PAGE and Western blotting were as

described previously (37). The antibodies used were anti-PDCD4 (Rockland), β-actin (Sigma), LF-113 (65), anti-human decorin (65), cleaved caspase-3, phosphorylated and total p44p42 and p38 (all from Cell Signaling). Protein bands were quantified using Scion image software (Scion Corporation). Quantification of decorin and cytokines in plasma, tissues, and cell culture supernatants was performed by ELISA (R&D Systems). The tissue ELISA measurements were normalized to the protein content of the homogenates (37).

Immunostaining

Formaldehyde-fixed and paraffin-embedded lungs and tumor tissues were processed for immunostaining as described previously (65). Primary antibodies included rabbit anti-murine decorin (LF-113) (65), rabbit anti-human PDCD4, and rat anti-mouse F4/80 (Serotec). Staining was visualized either by alkaline phosphatase anti-alkaline phosphatase (APAAP) or horseradish peroxidase technique. Counterstaining was with Meyer´s Hematoxylin (Sigma). Immunostaining specificity was confirmed by omitting the primary antibody and for decorin, staining of *Dcn*$^{-/-}$ tissue sections served as the negative control.

Cell culture and stimulation

Macrophages were harvested by peritoneal lavage, five days after i.p. injection of thioglycollate and cultured in RPMI 1640 (Invitrogen) as described previously (7). Peritoneal macrophages were obtained from *Dcn*$^{+/+}$, *Dcn*$^{-/-}$, C57BL/6, *Tlr2*$^{-/-}$, *Tlr4*$^{-/-}$, *Tlr2*$^{-/-}$ and *Tlr4-m* and *Il10*$^{-/-}$ mice and were stimulated with intact human decorin (8 μg/ml), LPS (100 ng/ml) and TGFβ1 (2 ng/ml, Sigma) at the indicated intervals. Macrophages (1.5×10^5/well in 96-well plates) were preincubated for 1 hour with 10 μM of MEK-1–2 inhibitor (U0126, Cell Signaling), p38 MAPK inhibitor (SB203580, Sigma), 60 ng/ml of anti-TGFβ1 (R&D Systems) compared to anti-IgG (Sigma), or for 30 min with tyrphostin AG1024 and AG1478 (both 10 μM, Alexis). In some experiments decorin (40 μg/ml) was immobilized on 96-well uncoated culture plates. Efficacy of decorin coating, which was determined with [^{35}S]sulfate labeled decorin, was 10%, similar to that shown previously for biglycan (7). Effects of coating on adherence of macrophages were excluded by an adhesion assay (CytoMatrix Cell Adhesion Assay, Millipore) and normalization of the results by the protein content of adherent macrophages. For transient transfection experiments, 2×10^5 macrophages per well (24-well plates) were transfected for 48 hours with small interfering RNA (siRNA) for PDCD4 (100 nM), non-targeting control siRNA (both Thermo Fisher Scientific), anti-miR™ miRNA-21 inhibitor (60 nM) and anti-miR™ negative control (all from Ambion/Applied Biosystems) using the HiPerfect Transfection Reagent (Qiagen) as per the manufacturer's instructions. After transfection, cells were stimulated with LPS (100 ng/ml) and decorin (8 μg/ml) for the indicated time points.

HEK293 cells stably coexpressing the human TLR2 or TLR4 gene and the NF-κB-inducible SEAP reporter gene (HEK-Blue™-hTLR2 and HEK-Blue™-hTLR4 cells, both from Invivogen), and HEK-Blue-Null1 (HEK-Null, Invivogen) cells were cultured in DMEM-Glutamax medium (Invitrogen) supplemented with 10% fetal calf serum (FCS), 100 units/ml penicillin, 100 μg/ml streptomycin, 100 μg/ml normocin, 1 mM-glutamine, and 1X HEK-Blue selection™ (Invivogen).

SEAP NF-κB activity assay

1×10^5 HEK-Blue-hTLR2, HEK-Blue-hTLR4, and HEK-Null cells containing the SEAP reporter gene (Invivogen) for monitoring the activation of the NF-κB pathway were used for the assay. Efficiency of transfection was measured by ELISAs for human TLR2 and TLR4 (both Biozol). To validate the specificity of the assay, HEK-Blue-hTLR2, HEK-Blue-hTLR4, and HEK-Null cells were additionally stimulated with the TLR2 ligand peptidoglycan (PGN, 5 μg/ml) and the TLR4 ligand LPS (100 ng/ml). Cells were stimulated with decorin (8 μg/ml) for 6 hours and the activation of TLR2 and TLR4 signaling was analyzed by measuring the secreted SEAP according to the manufacturer's instructions (Invivogen). Briefly, 20 μl of the culture medium were mixed with 180 μl QUANTI-Blue detection medium (Invivogen) and incubated for 30 min at 37°C. The presence of SEAP (purple-blue) was measured as absorbance at 655 nm.

Immunoprecipitation assay

Immunoprecipitation of decorin with TLR2 and TLR4 from HEK-Blue-hTLR2, HEK-Blue-hTLR4 and HEK-Null transfected cell lysates was performed using protein A-Agarose affinity chromatography matrix (Roche) immobilized with decorin and anti-decorin antibody complexes by means of an irreversible cross-linker (BS3, Thermo Scientific). Precleared HEK-Blue-hTLR2 and HEK-Blue-hTLR4 cell lysates were added to the decorin-coated beads and incubated overnight at 4°C on a rotor. The immunoprecipitated proteins were eluted and analyzed by SDS-PAGE and Western blotting. The membranes were incubated with anti-TLR2 (IMG-416A, Imgenex) and anti-TLR4 (IMG-577, Imgenex) followed by incubation with sheep anti-mouse-HRP (Abcam) or donkey anti rabbit-HRP (GE Healthcare) conjugate. For controls, a similar amount of protein A-Agarose was incubated: (i) without cross-linker, (ii) with the antibody and HEK-Blue-hTLR2 or -hTLR4 cell lysate and without decorin, and (iii) with the antibody and decorin in the presence or absence of HEK-Null cell lysates.

Assaying binding of TLR2 and TLR4 to decorin using microscale thermophoresis

Protein-protein interactions of decorin with recombinant human TLR2 or human TLR4 and MD2 complex (R&D Systems) were determined by changes in the thermophoretic movement of decorin labeled with the fluorophore NT-647 (Monolith NT™ protein Labeling Kit, NanoTemper Technologies) using the microscale thermophoresis binding assay (NanoTemper Technologies) (66). A titration series of TLR2 protein (1000 nM to 1.95 nM) and the complex of TLR4 and MD2 (350 nM to 0.68 nM) each diluted 1:1 with PBS containing 0.05% Tween 20 was performed. The concentration of NT-647-labeled decorin was kept constant (10 nM). The TLRs were incubated with decorin for 30 min in the dark to enable binding. The reaction was then aspirated into glass capillaries, sealed with wax and the thermophoretic movement of labeled decorin monitored with a laser on for 30 s and off for 5 s at a laser voltage of 60%. To demonstrate that the changed thermophoresis of decorin was actually due to its interaction with TLR2 or TLR4 and MD2 complex, NT-647-labeled albumin (10 nM, Thermo Fisher Scientific) was tested for its binding to TLR2 and TLR4 in the same experimental setting as negative control. Fluorescence was measured before laser heating ($F_{Initial}$) and after 30 s of laser on time (F_{Hot}). The normalized fluorescence F_{Norm} =

$F_{Hot}/F_{Initial}$ reflects the concentration ratio of labeled molecules. F_{norm} was plotted directly and multiplied by a factor of 10, yielding a relative change in fluorescence per mill. Kd was calculated from three independent thermophoresis measurements using NanoTemper Software (NanoTemper Technologies).

RNA isolation and qRT-PCR

Total RNA was isolated from tissues or cells using TRIzol reagent (Invitrogen) and mirVana miRNA isolation kit (Applied Biosystems) and cDNA was prepared using the Verso cDNA Kit (Thermo Fisher Scientific) and TaqMan MicroRNA Reverse Transcription Kit (Applied Biosystems). The following inventoried TaqMan assay probes for individual mRNAs were used: mouse *Dcn* (Mm00514535_m1), mouse *Pdcd4* (Mm01266062_m1), mouse *Tnf* (Mm00443258_m1), mouse *Il10* (Mm99999062_m1), mouse *Il12b* (Mm01288993_m1), mouse *Gapdh* (Mm03302249_g1), mouse *mmu-miR-21* (002493) and human *U6* (*RNU6B*) (001093). Change in the threshold method (ΔΔCt) was used to calculate and the results are represented as relative fold induction compared to the control sample and are normalized to the endogenous control RNU6B for miRNA analysis and *Gapdh* for gene-expression analysis.

Procedures to rule out contamination of decorin

Endotoxin contamination of decorin (1 μg/μl), after each purification step and in each new aliquot, was tested with the LAL kinetic chromogenic assay using the PTS™ Endosafe system (Charles River) at dilutions of 1:10-1:1000 in the presence of a LPS standard curve in a concentration range of 1 – 500 pg/ml. One unit of endotoxin per milliliter (EU/ml) equaled 50 – 100 pg endotoxin/ml. Accordingly, decorin concentrations of 8 μg/ml used in the experiments corresponded to 16 ± 4.0 pg/ml (n = 3) of LPS. Contaminations with endotoxin were additionally controlled by boiling decorin or LPS for 30 min in PBS buffer containing 2 mM dithiothreitol and 1 mM EDTA or by preincubation with polymyxin B (Sigma-Aldrich, 50 μg/ml, 1 hour) prior to incubation with macrophages or HEK-Blue-hTLR4 cells. Other contaminants have been rigorously excluded by several assays (7). Briefly, the purity of intact decorin and its protein core was verified by silver staining after SDS gel electrophoresis. Contamination of decorin with TNFα, IL-12, IL-10, TGF-β1, IL-6 or IL-1β was excluded by ELISAs (R&D Systems). Contamination with selective TLR2 and TLR4 ligands was excluded by Western blotting using 8–16 μg decorin followed by immunodetection with anti-HSP-60 (Imgenex), anti-HSP-70 (StressGen Biotechnologies), anti-fibronectin-extra domain A (Harlan Sera-Lab), and by the Hyaluronan DuoSet Assay Development kit (R&D Systems). Finally, 8 μg of decorin, chondroitin or dermatan sulfate (Medac), heparan sulfate (Seikagaku Corporation), and human umbilical cord hyaluronan (Sigma), respectively, were digested with protease-free chondroitinase ABC (Seikagaku Corporation). Progress of digestion was controlled by measuring the increase in absorbance at 232 nm. Efficiency of digestion of decorin with chondroitinase ABC and the persistence of its protein core were additionally tested by Western blotting using a monoclonal anti-proteoglycan Di-4S antibody (clone 2-B-6, Seikagaku Corporation) and anti-decorin, respectively. Decorin-derived GAG chains were obtained by β-elimination followed by dialysis against RPMI 1640 medium. For quantification, protein and hexuronic acid content in the GAG chains and intact decorin were measured (7). Activation of macrophages by

chondroitinase ABC-digested decorin or by decorin-derived GAG chains was tested in mouse TNFα and IL-12 ELISAs (R&D Systems).

Other procedures

Purification of human decorin from conditioned media of human fibroblasts was performed as described previously (65). Protein concentrations were determined using the BCA Protein Assay Reagent (Pierce).

Statistical analysis

Data are given as means ± SEM analyzed by one-way analysis of variance (ANOVA), with Dunnett's significance correction test (SPSS software). Differences were considered significant at P-values < 0.05.

Supplementary Material

Refer to Web version on PubMed Central for supplementary material.

Acknowledgments

This work was supported by the German Research Council (SFB 815, project A5, SCHA 1082/2-1, GRK 1172 and Excellence Cluster ECCPS to L.S.), Frankfurt International Research Graduate School for Translational Biomedicine (R.M. and L.S), and by NIH grants RO1 CA39481, RO1 CA47282 and RO1 CA120975 (RVI).

REFERENCES AND NOTES

1. Dunn GP, Old LJ, Schreiber RD. The immunobiology of cancer immunosurveillance and immunoediting. Immunity. 2004; 21:137. [PubMed: 15308095]
2. Hilliard A, Hilliard B, Zheng SJ, Sun H, Miwa T, Song W, Goke R, Chen YH. Translational regulation of autoimmune inflammation and lymphoma genesis by programmed cell death 4. J Immunol. 2006; 177:8095. [PubMed: 17114484]
3. Yasuda M, Schmid T, Rubsamen D, Colburn NH, Irie K, Murakami A. Downregulation of programmed cell death 4 by inflammatory conditions contributes to the generation of the tumor promoting microenvironment. Mol Carcinog. 2010; 49:837. [PubMed: 20607724]
4. Sheedy FJ, Palsson-McDermott E, Hennessy EJ, Martin C, O'Leary JJ, Ruan Q, Johnson DS, Chen Y, O'Neill LA. Negative regulation of TLR4 via targeting of the proinflammatory tumor suppressor PDCD4 by the microRNA miR-21. Nat Immunol. 2010; 11:141. [PubMed: 19946272]
5. Lankat-Buttgereit B, Goke R. The tumour suppressor Pdcd4: recent advances in the elucidation of function and regulation. Biol Cell. 2009; 101:309. [PubMed: 19356152]
6. Reis PP, Tomenson M, Cervigne NK, Machado J, Jurisica I, Pintilie M, Sukhai MA, Perez-Ordonez B, Grenman R, Gilbert RW, Gullane PJ, Irish JC, Kamel-Reid S. Programmed cell death 4 loss increases tumor cell invasion and is regulated by miR-21 in oral squamous cell carcinoma. Mol Cancer. 2010; 9:238. [PubMed: 20831814]
7. Schaefer L, Babelova A, Kiss E, Hausser HJ, Baliova M, Krzyzankova M, Marsche G, Young MF, Mihalik D, Gotte M, Malle E, Schaefer RM, Grone HJ. The matrix component biglycan is proinflammatory and signals through Toll-like receptors 4 and 2 in macrophages. J Clin Invest. 2005; 115:2223. [PubMed: 16025156]
8. Schaefer L, Macakova K, Raslik I, Micegova M, Grone HJ, Schonherr E, Robenek H, Echtermeyer FG, Grassel S, Bruckner P, Schaefer RM, Iozzo RV, Kresse H. Absence of decorin adversely influences tubulointerstitial fibrosis of the obstructed kidney by enhanced apoptosis and increased inflammatory reaction. Am J Pathol. 2002; 160:1181. [PubMed: 11891213]

9. Goldoni S, Iozzo RV. Tumor microenvironment: Modulation by decorin and related molecules harboring leucine-rich tandem motifs. Int J Cancer. 2008; 123:2473. [PubMed: 18798267]
10. Iozzo RV, Schaefer L. Proteoglycans in health and disease: novel regulatory signaling mechanisms evoked by the small leucine-rich proteoglycans. FEBS J. 2010; 277:3864. [PubMed: 20840584]
11. Kim YK, Kwon JT, Choi JY, Jiang HL, Arote R, Jere D, Je YH, Cho MH, Cho CS. Suppression of tumor growth in xenograft model mice by programmed cell death 4 gene delivery using folate-PEG-baculovirus. Cancer Gene Ther. 2010; 17:751. [PubMed: 20539318]
12. Yang HS, Jansen AP, Komar AA, Zheng X, Merrick WC, Costes S, Lockett SJ, Sonenberg N, Colburn NH. The transformation suppressor Pdcd4 is a novel eukaryotic translation initiation factor 4A binding protein that inhibits translation. Mol Cell Biol. 2003; 23:26. [PubMed: 12482958]
13. Dorrello NV, Peschiaroli A, Guardavaccaro D, Colburn NH, Sherman NE, Pagano M. S6K1- and betaTRCP-mediated degradation of PDCD4 promotes protein translation and cell growth. Science. 2006; 314:467. [PubMed: 17053147]
14. Asangani IA, Rasheed SA, Nikolova DA, Leupold JH, Colburn NH, Post S, Allgayer H. MicroRNA-21 (miR-21) post-transcriptionally downregulates tumor suppressor Pdcd4 and stimulates invasion, intravasation and metastasis in colorectal cancer. Oncogene. 2008; 27:2128. [PubMed: 17968323]
15. Allgayer H. Pdcd4, a colon cancer prognostic that is regulated by a microRNA. Crit Rev Oncol Hematol. 2010; 73:185. [PubMed: 19836969]
16. Roa W, Brunet B, Guo L, Amanie J, Fairchild A, Gabos Z, Nijjar T, Scrimger R, Yee D, Xing J. Identification of a new microRNA expression profile as a potential cancer screening tool. Clin Invest Med. 2010; 33:E124. [PubMed: 20370992]
17. Hatley ME, Patrick DM, Garcia MR, Richardson JA, Bassel-Duby R, van Rooij E, Olson EN. Modulation of K-Ras-dependent lung tumorigenesis by MicroRNA-21. Cancer Cell. 2010; 18:282. [PubMed: 20832755]
18. Davis BN, Hilyard AC, Lagna G, Hata A. SMAD proteins control DROSHA-mediated microRNA maturation. Nature. 2008; 454:56. [PubMed: 18548003]
19. Yao Q, Cao S, Li C, Mengesha A, Kong B, Wei M. Micro-RNA-21 regulates TGF-beta-induced myofibroblast differentiation by targeting PDCD4 in tumor-stroma interaction. Int J Cancer. 2011; 128:1783. [PubMed: 20533548]
20. Goldoni S, Seidler DG, Heath J, Fassan M, Baffa R, Thakur ML, Owens RT, McQuillan DJ, Iozzo RV. An antimetastatic role for decorin in breast cancer. Am J Pathol. 2008; 173:844. [PubMed: 18688028]
21. Sorokin L. The impact of the extracellular matrix on inflammation. Nat Rev Immunol. 2010; 10:712. [PubMed: 20865019]
22. Grivennikov SI, Greten FR, Karin M. Immunity, inflammation, and cancer. Cell. 2010; 140:883. [PubMed: 20303878]
23. Schaefer L. Extracellular matrix molecules: endogenous danger signals as new drug targets in kidney diseases. Curr Opin Pharmacol. 2010; 10:185. [PubMed: 20045380]
24. Chen GY, Nunez G. Sterile inflammation: sensing and reacting to damage. Nat Rev Immunol. 2010; 10:826. [PubMed: 21088683]
25. Border WA, Noble NA, Yamamoto T, Harper JR, Yamaguchi Y, Pierschbacher MD, Ruoslahti E. Natural inhibitor of transforming growth factor-beta protects against scarring in experimental kidney disease. Nature. 1992; 360:361. [PubMed: 1280332]
26. Yamaguchi Y, Mann DM, Ruoslahti E. Negative regulation of transforming growth factor-beta by the proteoglycan decorin. Nature. 1990; 346:281. [PubMed: 2374594]
27. Koninger J, Giese NA, Bartel M, di Mola FF, Berberat PO, di Sebastiano P, Giese T, Buchler MW, Friess H. The ECM proteoglycan decorin links desmoplasia and inflammation in chronic pancreatitis. J Clin Pathol. 2006; 59:21. [PubMed: 16394277]
28. Xaus J, Comalada M, Cardo M, Valledor AF, Celada A. Decorin inhibits macrophage colony-stimulating factor proliferation of macrophages and enhances cell survival through induction of p27(Kip1) and p21(Waf1). Blood. 2001; 98:2124. [PubMed: 11567999]

29. Comalada M, Cardo M, Xaus J, Valledor AF, Lloberas J, Ventura F, Celada A. Decorin reverses the repressive effect of autocrine-produced TGF-beta on mouse macrophage activation. J Immunol. 2003; 170:4450. [PubMed: 12707320]
30. Berg DJ, Kuhn R, Rajewsky K, Muller W, Menon S, Davidson N, Grunig G, Rennick D. Interleukin-10 is a central regulator of the response to LPS in murine models of endotoxic shock and the Shwartzman reaction but not endotoxin tolerance. J Clin Invest. 1995; 96:2339. [PubMed: 7593621]
31. Shimazu R, Akashi S, Ogata H, Nagai Y, Fukudome K, Miyake K, Kimoto M. MD-2, a molecule that confers lipopolysaccharide responsiveness on Toll-like receptor 4. J Exp Med. 1999; 189:1777. [PubMed: 10359581]
32. Kawai T, Akira S. The role of pattern-recognition receptors in innate immunity: update on Toll-like receptors. Nat Immunol. 2010; 11:373. [PubMed: 20404851]
33. Tralhao JG, Schaefer L, Micegova M, Evaristo C, Schonherr E, Kayal S, Veiga-Fernandes H, Danel C, Iozzo RV, Kresse H, Lemarchand P. In vivo selective and distant killing of cancer cells using adenovirus-mediated decorin gene transfer. FASEB J. 2003; 17:464. [PubMed: 12631584]
34. Seidler DG, Goldoni S, Agnew C, Cardi C, Thakur ML, Owens RT, McQuillan DJ, Iozzo RV. Decorin protein core inhibits in vivo cancer growth and metabolism by hindering epidermal growth factor receptor function and triggering apoptosis via caspase-3 activation. J Biol Chem. 2006; 281:26408. [PubMed: 16835231]
35. Strazynski M, Eble JA, Kresse H, Schonherr E. Interleukin (IL)-6 and IL-10 induce decorin mRNA in endothelial cells, but interaction with fibrillar collagen is essential for its translation. J Biol Chem. 2004; 279:21266. [PubMed: 15016829]
36. Babelova A, Moreth K, Tsalastra-Greul W, Zeng-Brouwers J, Eickelberg O, Young MF, Bruckner P, Pfeilschifter J, Schaefer RM, Grone HJ, Schaefer L. Biglycan, a danger signal that activates the NLRP3 inflammasome via toll-like and P2X receptors. J Biol Chem. 2009; 284:24035. [PubMed: 19605353]
37. Moreth K, Brodbeck R, Babelova A, Gretz N, Spieker T, Zeng-Brouwers J, Pfeilschifter J, Young MF, Schaefer RM, Schaefer L. The proteoglycan biglycan regulates expression of the B cell chemoattractant CXCL13 and aggravates murine lupus nephritis. J Clin Invest. 2010; 120:4251. [PubMed: 21084753]
38. Taylor KR, Gallo RL. Glycosaminoglycans and their proteoglycans: host-associated molecular patterns for initiation and modulation of inflammation. FASEB J. 2006; 20:9. [PubMed: 16394262]
39. Coll RC, O'Neill LA. New insights into the regulation of signalling by toll-like receptors and nod-like receptors. J Innate Immun. 2010; 2:406. [PubMed: 20505309]
40. Schonherr E, Broszat M, Brandan E, Bruckner P, Kresse H. Decorin core protein fragment Leu155-Val260 interacts with TGF-beta but does not compete for decorin binding to type I collagen. Arch Biochem Biophys. 1998; 355:241. [PubMed: 9675033]
41. Hildebrand A, Romaris M, Rasmussen LM, Heinegard D, Twardzik DR, Border WA, Ruoslahti E. Interaction of the small interstitial proteoglycans biglycan, decorin and fibromodulin with transforming growth factor beta. Biochem J. 1994; 302(Pt 2):527. [PubMed: 8093006]
42. Merline R, Schaefer RM, Schaefer L. The matricellular functions of small leucine-rich proteoglycans (SLRPs). J Cell Commun Signal. 2009; 3:323. [PubMed: 19809894]
43. Cassatella MA, Meda L, Gasperini S, Calzetti F, Bonora S. Interleukin 10 (IL-10) upregulates IL-1 receptor antagonist production from lipopolysaccharide-stimulated human polymorphonuclear leukocytes by delaying mRNA degradation. J Exp Med. 1994; 179:1695. [PubMed: 8163946]
44. D'Andrea A, Aste-Amezaga M, Valiante NM, Ma X, Kubin M, Trinchieri G. Interleukin 10 (IL-10) inhibits human lymphocyte interferon gamma-production by suppressing natural killer cell stimulatory factor/IL-12 synthesis in accessory cells. J Exp Med. 1993; 178:1041. [PubMed: 8102388]
45. Frankel LB, Christoffersen NR, Jacobsen A, Lindow M, Krogh A, Lund AH. Programmed cell death 4 (PDCD4) is an important functional target of the microRNA miR-21 in breast cancer cells. J Biol Chem. 2008; 283:1026. [PubMed: 17991735]

46. Cabello-Verrugio C, Brandan E. A novel modulatory mechanism of transforming growth factor-beta signaling through decorin and LRP-1. J Biol Chem. 2007; 282:18842. [PubMed: 17485468]
47. Min KM, Kim PH. Macrophage-derived TGF-beta1 induces IgA isotype expression. Mol Cells. 2003; 16:245. [PubMed: 14651268]
48. Seki E, De Minicis S, Osterreicher CH, Kluwe J, Osawa Y, Brenner DA, Schwabe RF. TLR4 enhances TGF-beta signaling and hepatic fibrosis. Nat Med. 2007; 13:1324. [PubMed: 17952090]
49. Stander M, Naumann U, Wick W, Weller M. Transforming growth factor-beta and p-21: multiple molecular targets of decorin-mediated suppression of neoplastic growth. Cell Tissue Res. 1999; 296:221. [PubMed: 10382266]
50. Iwashita Y, Ogawa T, Goto S, Nakanishi M, Goto T, Kitano S. Effective transfer of interleukin-12 gene to solid tumors using a novel gene delivery system, poly [D,L-2,4-diaminobutyric acid]. Cancer Gene Ther. 2004; 11:103. [PubMed: 14671674]
51. Eisenring M, Vom Berg J, Kristiansen G, Saller E, Becher B. IL-12 initiates tumor rejection via lymphoid tissue-inducer cells bearing the natural cytotoxicity receptor NKp46. Nat Immunol. 2010; 11:1030. [PubMed: 20935648]
52. Jarnicki AG, Lysaght J, Todryk S, Mills KH. Suppression of antitumor immunity by IL-10 and TGF-beta-producing T cells infiltrating the growing tumor: influence of tumor environment on the induction of CD4+ and CD8+ regulatory T cells. J Immunol. 2006; 177:896. [PubMed: 16818744]
53. Yingling JM, Blanchard KL, Sawyer JS. Development of TGF-beta signalling inhibitors for cancer therapy. Nat Rev Drug Discov. 2004; 3:1011. [PubMed: 15573100]
54. Troup S, Njue C, Kliewer EV, Parisien M, Roskelley C, Chakravarti S, Roughley PJ, Murphy LC, Watson PH. Reduced expression of the small leucine-rich proteoglycans, lumican, and decorin is associated with poor outcome in node-negative invasive breast cancer. Clin Cancer Res. 2003; 9:207. [PubMed: 12538471]
55. Matsumine A, Shintani K, Kusuzaki K, Matsubara T, Satonaka H, Wakabayashi T, Iino T, Uchida A. Expression of decorin, a small leucine-rich proteoglycan, as a prognostic factor in soft tissue tumors. J Surg Oncol. 2007; 96:411. [PubMed: 17579351]
56. Gu Y, Zhang S, Wu Q, Xu S, Cui Y, Yang Z, Zhao X, Sun B. Differential expression of decorin, EGFR and cyclin D1 during mammary gland carcinogenesis in TA2 mice with spontaneous breast cancer. J Exp Clin Cancer Res. 2010; 29:6. [PubMed: 20092659]
57. Bitomsky N, Wethkamp N, Marikkannu R, Klempnauer KH. siRNA-mediated knockdown of Pdcd4 expression causes upregulation of p21(Waf1/Cip1) expression. Oncogene. 2008; 27:4820. [PubMed: 18427550]
58. Iozzo RV, Sanderson RD. Proteoglycans in Cancer Biology, Tumor Microenvironment and Angiogenesis. J Cell Mol Med. 2010
59. Theocharis AD, Skandalis SS, Tzanakakis GN, Karamanos NK. Proteoglycans in health and disease: novel roles for proteoglycans in malignancy and their pharmacological targeting. FEBS J. 2010; 277:3904. [PubMed: 20840587]
60. Goldoni S, Humphries A, Nystrom A, Sattar S, Owens RT, McQuillan DJ, Ireton K, Iozzo RV. Decorin is a novel antagonistic ligand of the Met receptor. J Cell Biol. 2009; 185:743. [PubMed: 19433454]
61. Hu Y, Sun H, Owens RT, Wu J, Chen YQ, Berquin IM, Perry D, O'Flaherty JT, Edwards IJ. Decorin suppresses prostate tumor growth through inhibition of epidermal growth factor and androgen receptor pathways. Neoplasia. 2009; 11:1042. [PubMed: 19794963]
62. Buraschi S, Pal N, Tyler-Rubinstein N, Owens RT, Neill T, Iozzo RV. Decorin antagonizes Met receptor activity and down-regulates {beta}-catenin and Myc levels. J Biol Chem. 2010; 285:42075. [PubMed: 20974860]
63. Bone RC, Balk RA, Cerra FB, Dellinger RP, Fein AM, Knaus WA, Schein RM, Sibbald WJ. Definitions for sepsis and organ failure and guidelines for the use of innovative therapies in sepsis. The ACCP/SCCM Consensus Conference Committee. American College of Chest Physicians/ Society of Critical Care Medicine. Chest. 1992; 101:1644. [PubMed: 1303622]
64. Knaus WA, Draper EA, Wagner DP, Zimmerman JE. APACHE II: a severity of disease classification system. Crit Care Med. 1985; 13:818. [PubMed: 3928249]

65. Schaefer L, Tsalastra W, Babelova A, Baliova M, Minnerup J, Sorokin L, Grone HJ, Reinhardt DP, Pfeilschifter J, Iozzo RV, Schaefer RM. Decorin-mediated regulation of fibrillin-1 in the kidney involves the insulin-like growth factor-I receptor and Mammalian target of rapamycin. Am J Pathol. 2007; 170:301. [PubMed: 17200203]

66. Wienken CJ, Baaske P, Rothbauer U, Braun D, Duhr S. Protein-binding assays in biological liquids using microscale thermophoresis. Nat Commun. 2010; 1:100. [PubMed: 20981028]

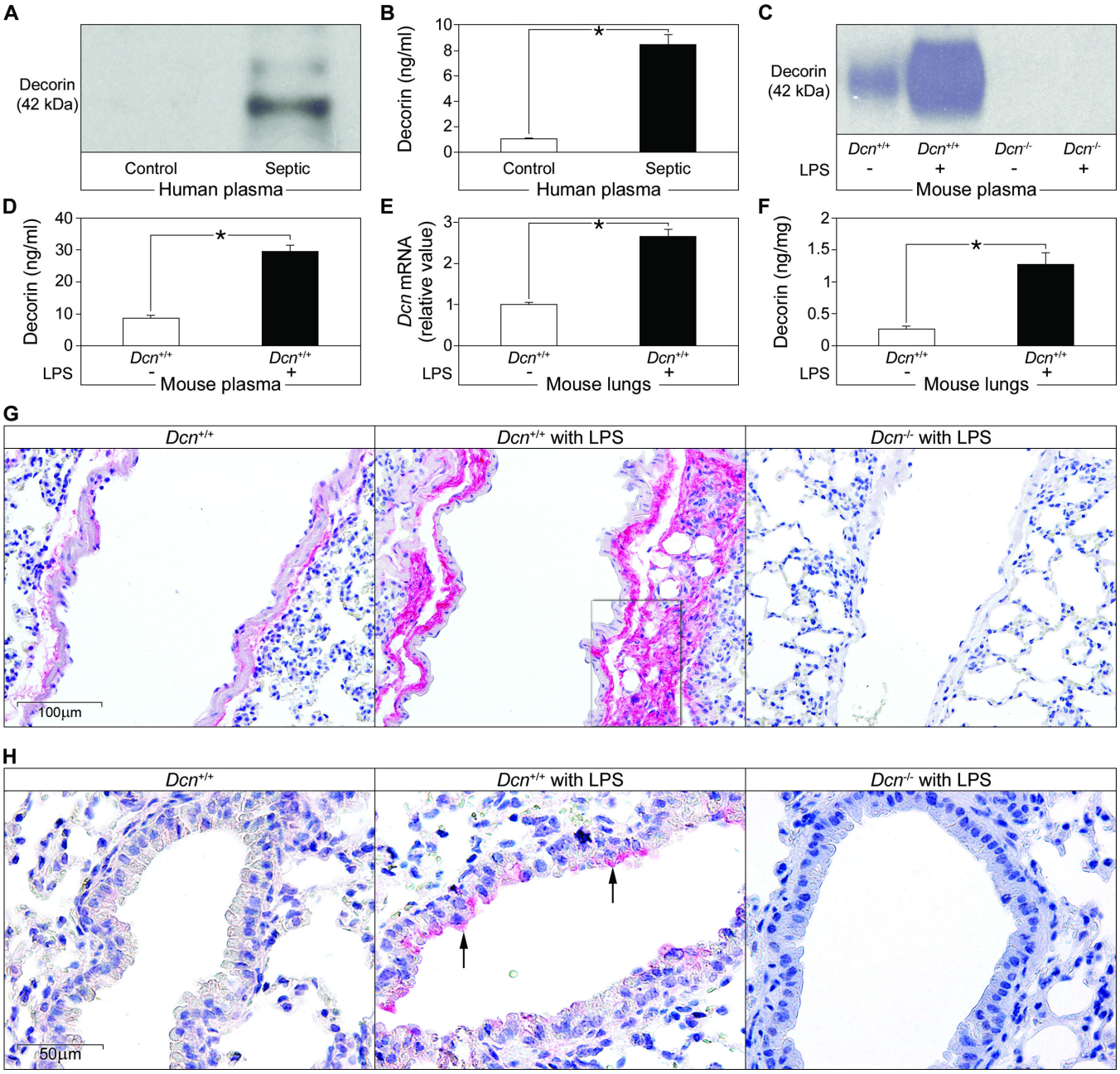

Fig. 1. Decorin concentrations are increased in plasma and lungs during sepsis

(**A**) Representative immunoblots of the decorin protein core in plasma from septic individuals (n = 15) and controls (n = 10). (**B**) ELISA of human decorin in the samples from (A). (**C** to **F**) Septic (induced by LPS) and control *Dcn*$^{+/+}$ and *Dcn*$^{-/-}$ mice were analyzed for plasma abundance of decorin protein core by immunoblot (C) and ELISA (D), *Dcn* mRNA abundance in septic lungs (normalized to *Gapdh*) by qPCR (E), and decorin abundance in lungs by ELISA (F). *n* = 12 septic mice or 6 control mice. Data represent the mean ±SEM (B, D-F). *P<0.05. (**G** and **H**) Immunohistochemical analysis of decorin (red) in perivascular regions (G) and in bronchial epithelial cells (arrows in H) as indicated. The

marked perivascular region in (G) was additionally double-stained for decorin and the macrophage marker F4/80) as shown in fig. S1A.

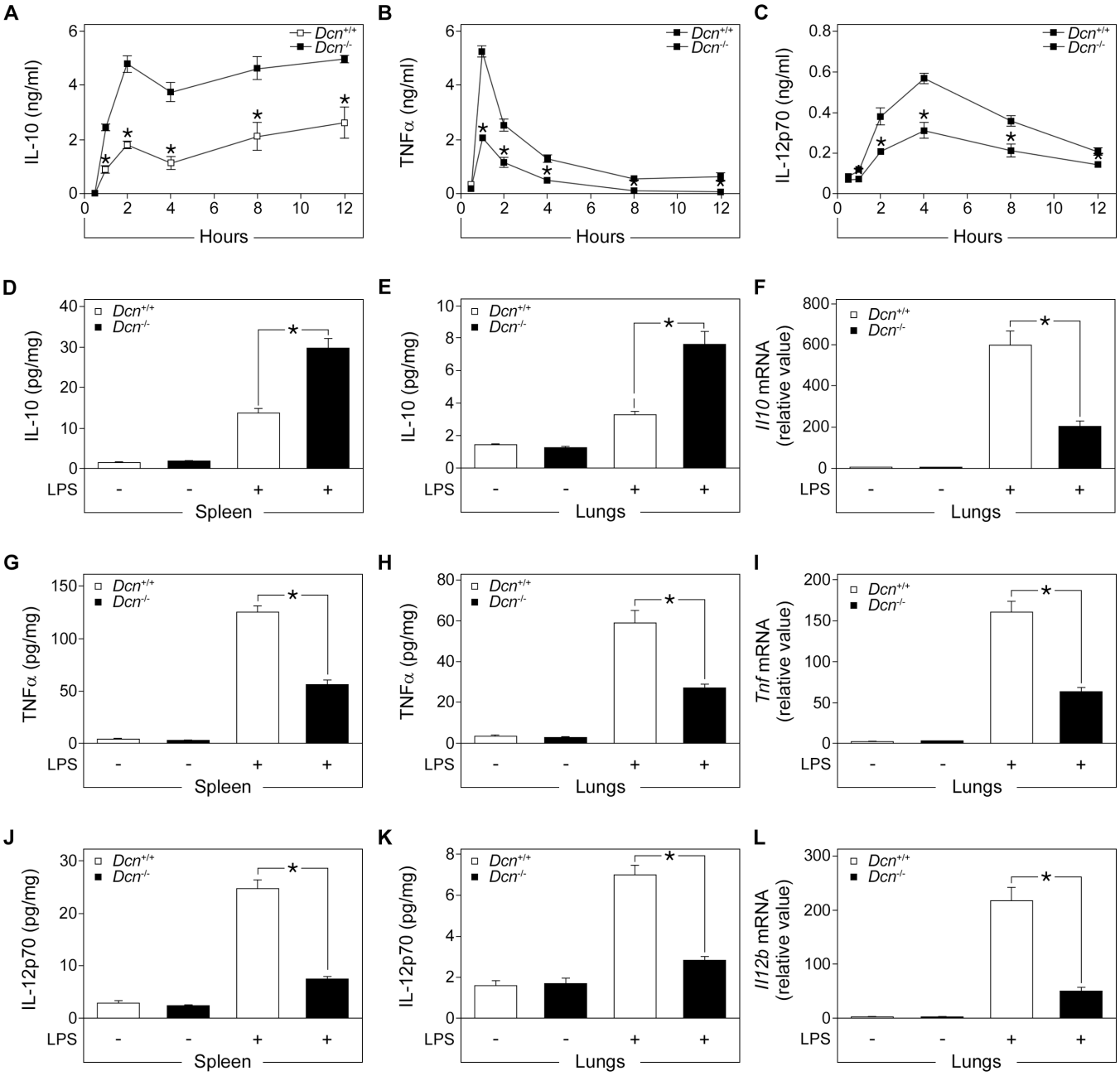

Fig. 2. Decorin deficiency increases IL-10 concentration and reduces TNFα and IL-12p70 concentrations in tissues and plasma from LPS-septic mice

Sepsis was induced in $Dcn^{+/+}$ and $Dcn^{-/-}$ mice by LPS injection. (**A** to **C**) Time course of IL-10 (A), TNFα (B), and IL-12p70 (C) amounts in plasma samples from septic $Dcn^{-/-}$ and $Dcn^{+/+}$ mice after LPS injection as measured by ELISA. Data represent the mean ±SEM. n = 3 mice/group. (**D** to **F**) IL-10 concentrations in spleen (D) and lungs (E) were determined by ELISA and *Il10* abundance determined by qPCR (F). (**G** to **I**) TNF-α concentrations in spleen (G) and lungs (H) were determined by ELISA and *Tnf* abundance determined by qPCR (I). (**J** to **L**) IL-12p70 concentrations in spleen (J) and lungs (K) were determined by ELISA and *Il12b* abundance determined by qPCR (L). qPCR data is presented as fold

induction normalized to *Gapdh*. Data represent the mean ±SEM. $n \geq 12$ in each group. *P<0.05.

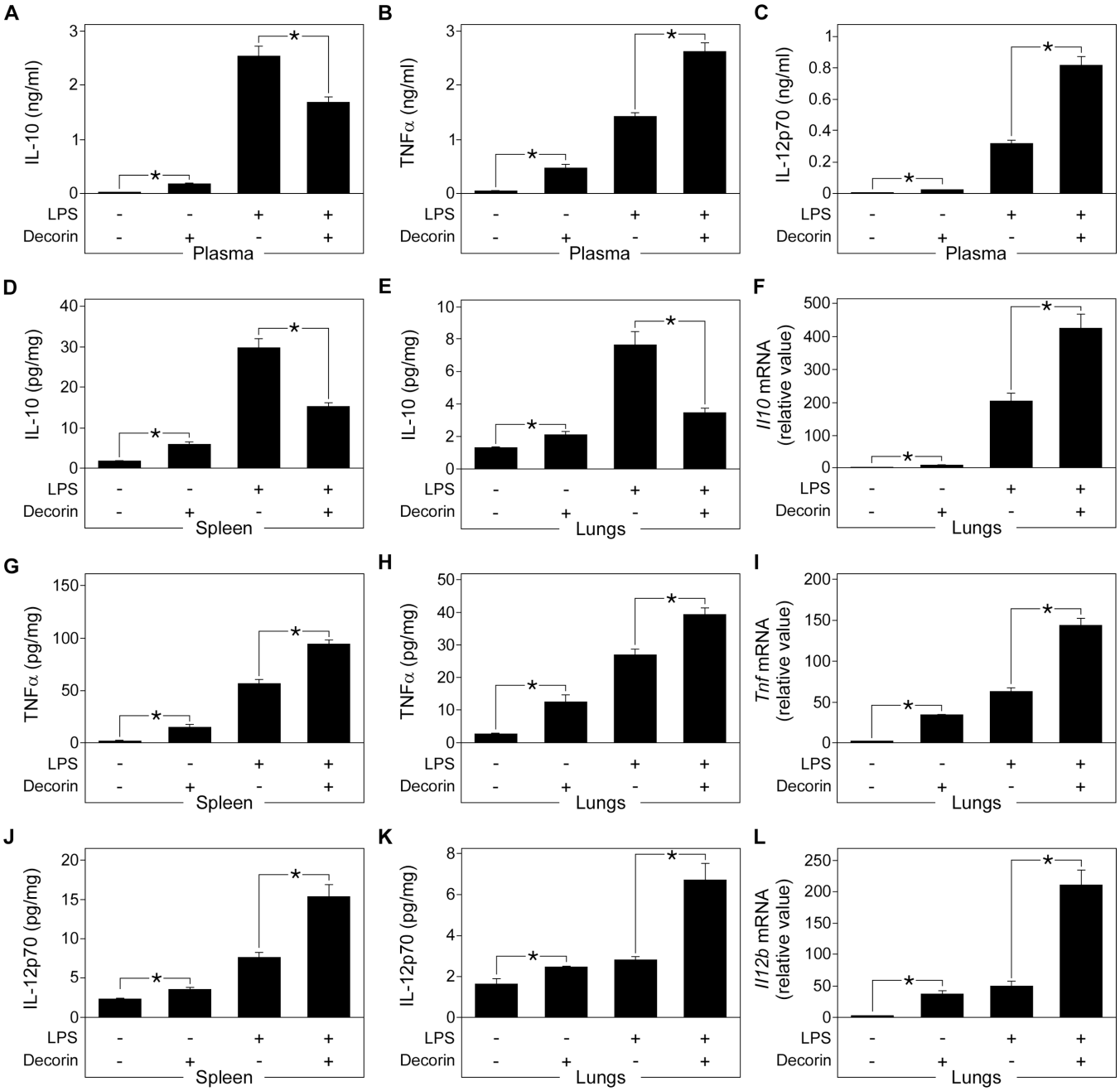

Fig. 3. Effects of exogenous decorin on IL-10, TNFα, and IL-12p70 protein and mRNA abundance in septic mice

Dcn$^{-/-}$ mice were injected with LPS to induce sepsis, then administered recombinant human decorin. (**A** to **C**) Plasma concentrations of IL-10 (A), TNFα (B), and IL-12p70 (C) in septic *Dcn*$^{-/-}$ and decorin-treated septic *Dcn*$^{-/-}$ mice were determined by ELISA. (**D** to **F**) IL-10 concentrations in spleen (D) and lungs (E) were determined by ELISA and *Il10* abundance determined by qPCR (F). (**G** to **I**) TNFα concentrations in spleen (G) and lungs (H) were determined by ELISA and *Tnf* abundance determined by qPCR (I). (**J** to **L**) IL-12p70 concentrations in spleen (J) and lungs (K) were determined by ELISA and *Il12b*

abundance determined by qPCR (L). qPCR data is presented as fold induction normalized to *Gapdh*. Data represent the mean ±SEM. $n = 6$ for decorin-treated septic $Dcn^{-/-}$ mice and $n \geq 12$ for other groups. *P<0.05.

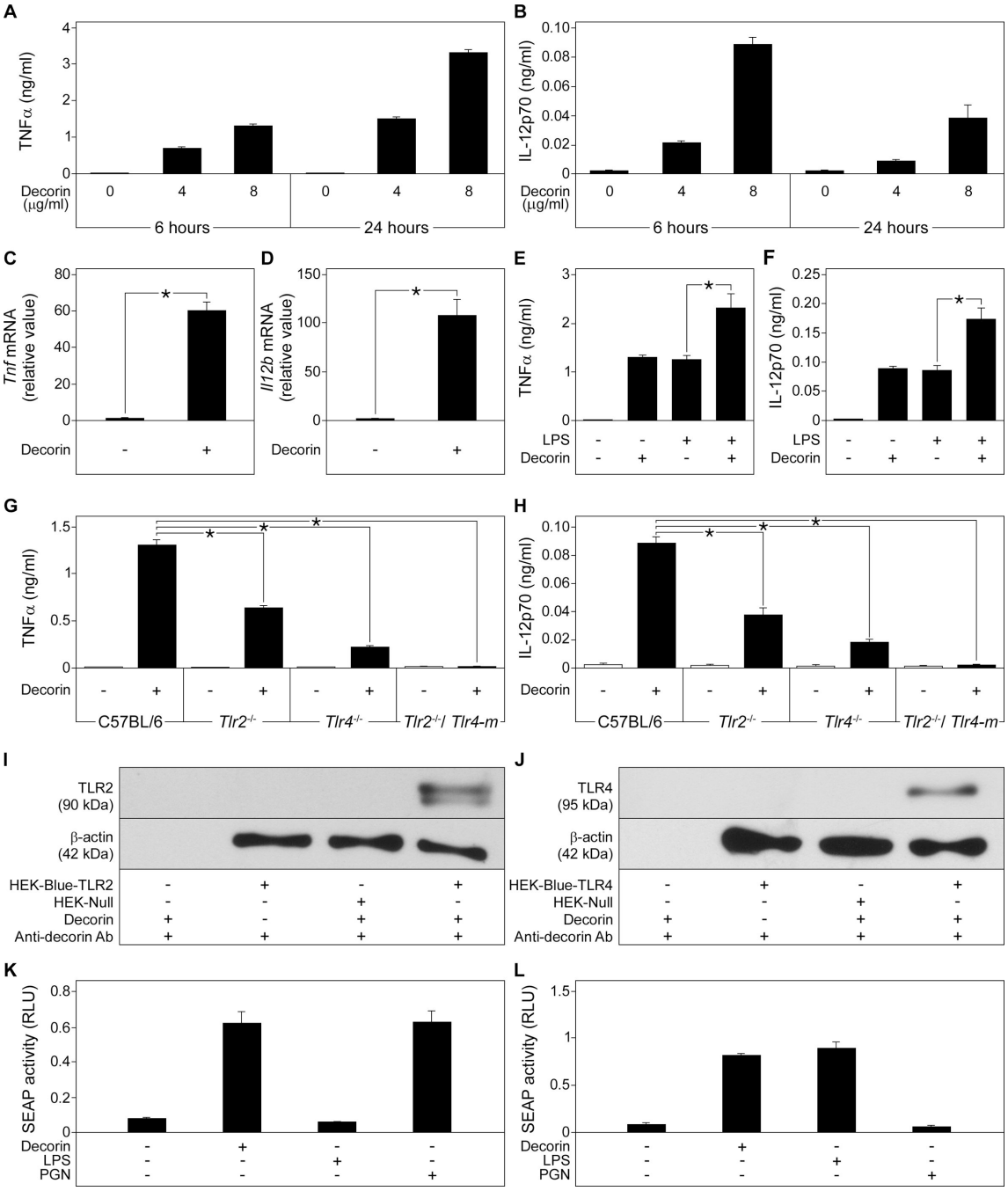

Fig. 4. Decorin induces TNFα and IL-12p70 release in macrophages through interaction with TLR2 and TLR4

(**A** and **B**) *Dcn*$^{+/+}$ macrophages were stimulated with decorin and the concentration of TNFα (A) and IL-12p70 (B) released into the media was measured by ELISA. (**C** and **D**) qPCR of *Tnf* (C) and *Il12b* (D) in decorin-stimulated *Dcn*$^{+/+}$ macrophages, presented as fold induction normalized to *Gapdh*. (**E** and **F**) *Dcn*$^{+/+}$ macrophages were stimulated with LPS, decorin, or both and the concentration of TNFα (E) and IL-12p70 (F) released into the media was measured by ELISA. (**G** and **H**) C57BL/6, *Tlr2*$^{-/-}$, *Tlr4*$^{-/-}$, *Tlr2*$^{-/-}$ and *Tlr4-m*

macrophages were cultured in the absence or presence of decorin and TNFα (G) and IL-12p70 (H) released into the media was measured by ELISA. (**I** and **J**) Western blots showing immunoprecipitation of TLR2 (I) and TLR4 (J) from HEK-Blue-hTLR2, HEK-Blue-hTLR4, and HEK-Null cells with decorin (top panels). β-actin served as the loading control (lower panels). (**K** and **L**) Activity in relative light units (RLU) of the NF-κB reporter gene SEAP in HEK-Blue-hTLR2 (K) and in HEK-Blue-hTLR4 (L) cells stimulated with decorin, LPS, or peptidoglycan. Data represent the mean ±SEM. $n \geq 3$ experiments. *P<0.05.

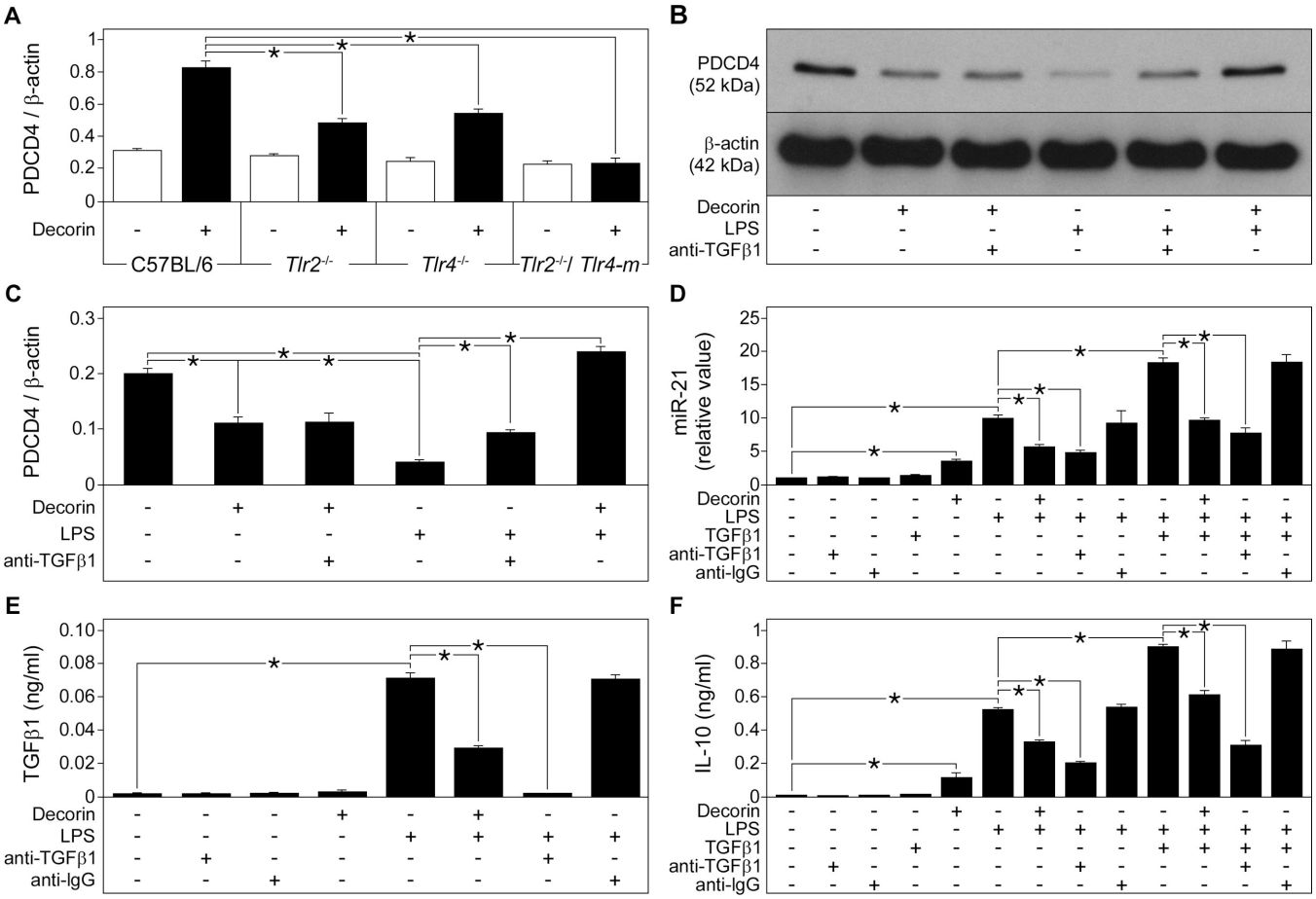

Fig. 5. Decorin increases PDCD4 abundance in macrophages through TLR2- and TLR4-dependent synthesis and through inhibition of TGFβ1-induced processing of miR-21

(**A**) Quantification of Western blots for PDCD4 normalized to β-actin in C57BL/6, *Tlr2*$^{-/-}$, *Tlr4*$^{-/-}$, and *Tlr2*$^{-/-}$/*Tlr4-m* macrophages stimulated with decorin. (**B** and **C**) Representative Western blots (B) and quantification (C) of PDCD4 normalized to β-actin in C57BL/6 macrophages stimulated with decorin, LPS, or both in the presence of a TGFβ1-neutralizing antibody. (**D**) qPCR of miR-21 in C57BL/6 macrophages preincubated with TGFβ1-neutralizing or anti-IgG antibodies, then stimulated with decorin, LPS or TGFβ1. Data are calculated as fold induction normalized to *RNU6B*. (**E** and **F**) ELISA for active TGFβ1 (E) and IL-10 (F) in media from C57BL/6 macrophages stimulated as described in (D). Data represent the mean ±SEM. $n \geq 3$ experiments. *P<0.05.

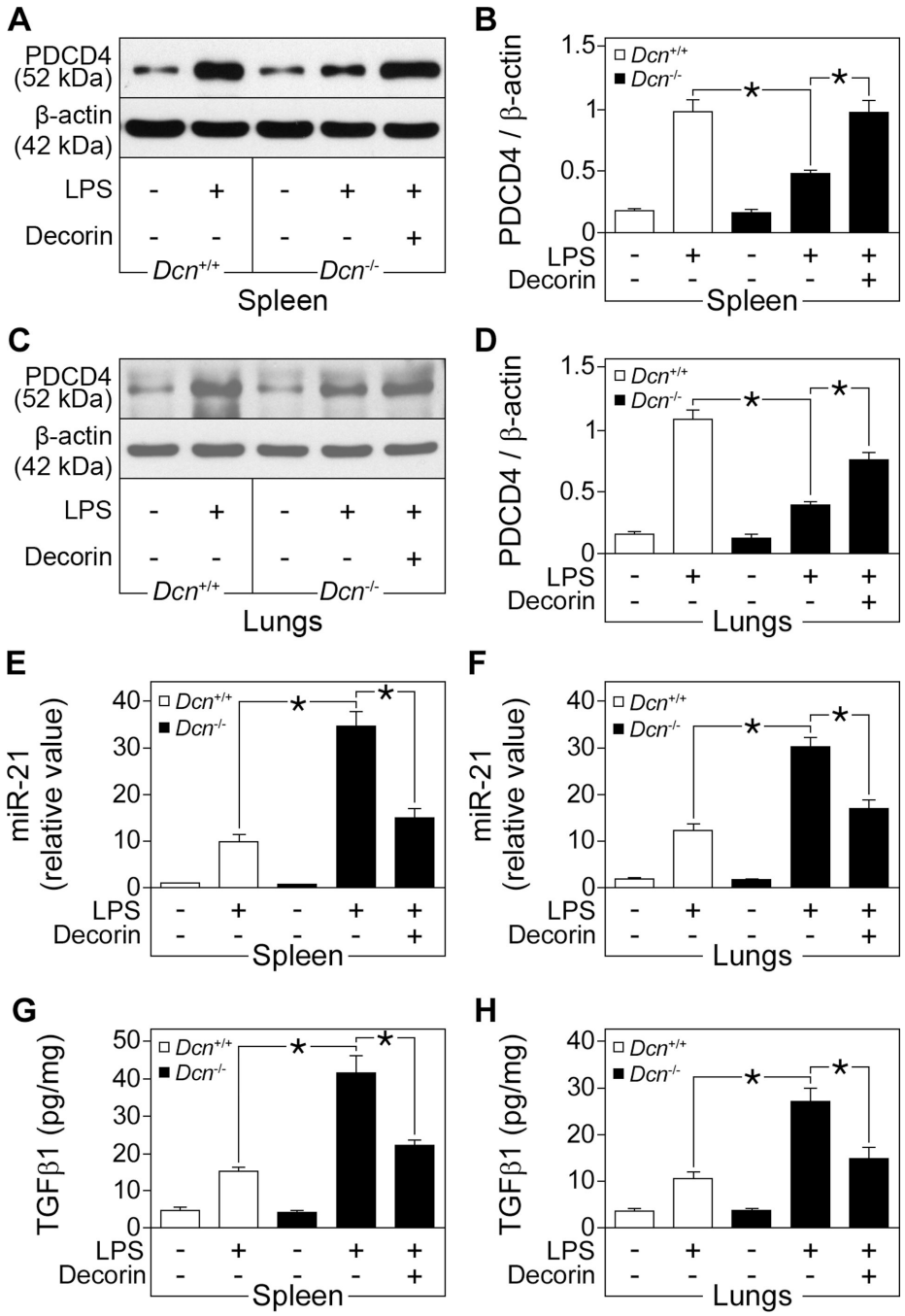

Fig. 6. Effects of decorin on the abundance of PDCD4, miR-21 and active TGFβ1 in LPS-induced septic mice

Dcn$^{+/+}$ and *Dcn*$^{-/-}$ mice were injected with LPS to induce sepsis, then administered recombinant human decorin. (**A** to **D**) Representative Western blots and quantification of PDCD4 normalized to β-actin in the spleen (A and B) and lungs (C and D). (**E** and **F**) qPCR of mouse miR-21 in the spleen (E) and lungs (F), presented as fold induction normalized to *RNU6B*. (**G** and **H**) Tissue cytokine ELISA for active murine TGFβ1 in the spleen (G) and

lungs (H). Data represent the mean ±SEM. $n = 6$ for decorin-treated septic $Dcn^{-/-}$ mice and $n \geq 12$ for other groups. *P<0.05.

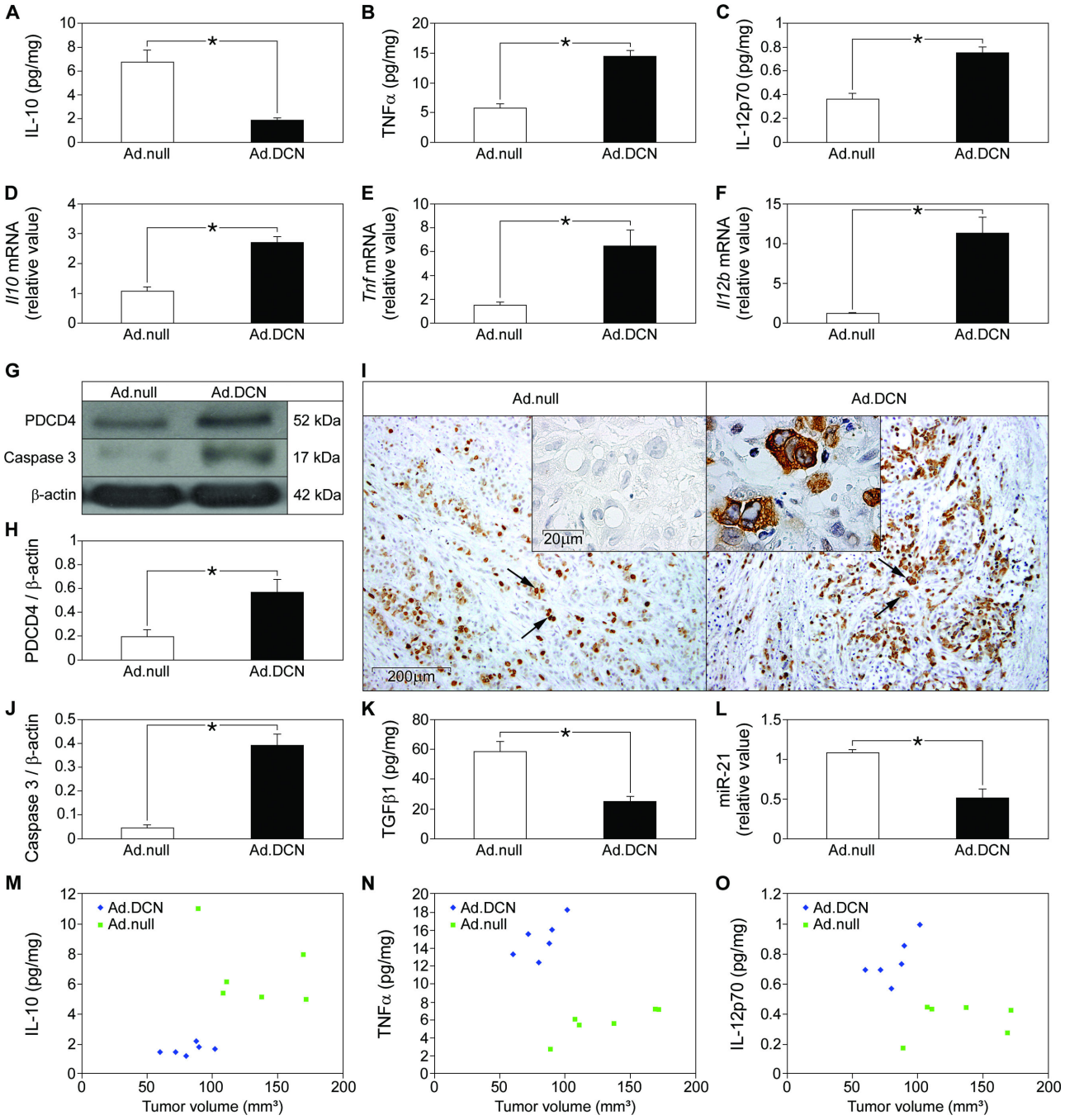

Fig. 7. Induction of proinflammatory immune response through inhibition of TGFβ1, downregulation of miR-21, and increased PDCD4 abundance in tumor xenografts overexpressing decorin

(**A** to **C**) Tumor xenografts in *nu*/*nu* mice were injected with Ad.DCN or Ad.null vector and the xenograft concentrations of IL-10 (A), TNFα (B), and IL-12p70 (C) were measured by ELISA. (**D** to **F**) qPCR of tumor xenograft mRNA for murine *Il10* (D), *Tnf* (E), and *Il12b* (F) presented as fold induction normalized to *Gapdh*. (**G**) Representative Western blots for murine and human PDCD4 and cleaved murine caspase-3 (active) in Ad.null and Ad.DCN injected tumor xenografts, normalized to β-actin for quantification (H, for PDCD4 and J, for

caspase 3). (**I**) Immunostaining for murine and human PDCD4 (brown) in sections of Ad.null- and Ad.DCN-injected tumors. Insert in Ad.null shows the no primary antibody control. Arrows in Ad.null and Ad.DCN and insert in Ad.DCN indicate cells stained for PDCD4. (**K**) Tumor tissue ELISA detecting active murine and human TGFβ1. (**L**) qPCR for murine miR-21 presented as fold induction normalized to *RNU6B*. (**M** to **O**) Association between tumor volume and amounts of IL-10 (M), TNFα (N), and IL-12p70 (O) in tumors injected with Ad.DCN or Ad.null vector. Data represent the mean ±SEM. $n \geq 6$ in each group. *P<0.05.

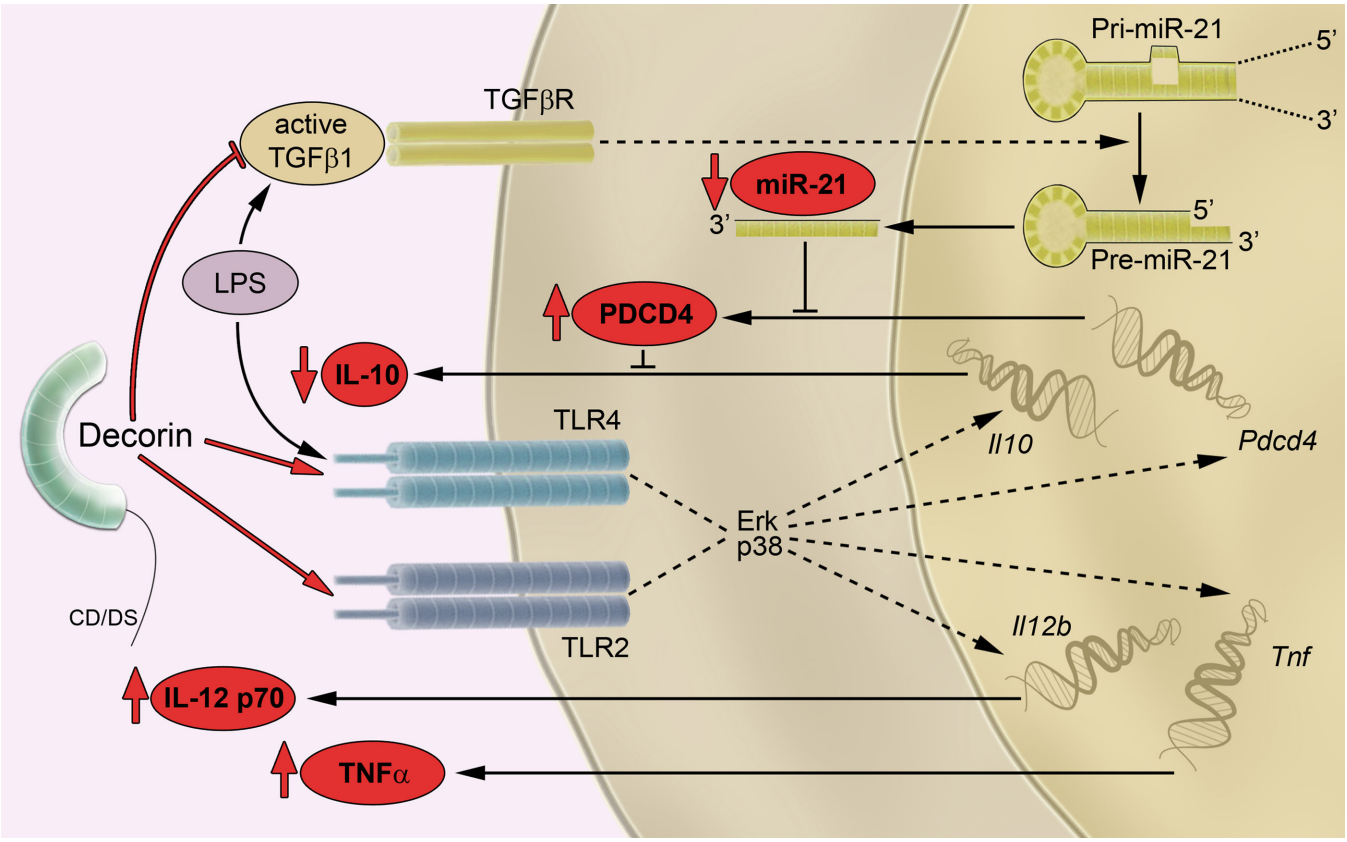

Fig. 8. A model of decorin-driven proinflammatory signaling

Decorin binds to TLR2 and TLR4, activates ERK and p38 MAPKs, and induces expression of *Il12b, Tnf, Il10*, and *Pdcd4*. Decorin- or LPS-mediated induction of PDCD4 leads to translational repression of IL-10. Furthermore, LPS induces the production of active TGFβ1, which promotes the processing of primary (pri-miR-21) to precursor (pre-miR-21) and increases the abundance of mature miR-21, a posttranscriptional inhibitor of PDCD4. Reduced PDCD4 abundance results in increased IL-10 release. In contrast, decorin inhibits TGFβ1 signaling, which subsequently leads to decreased miR-21 abundance and reduced IL-10 release. Thus, in the presence of LPS, decorin stimulates the expression of *Pdcd4* through TLR2 and inhibits the activity of TGFβ1 whose production had been induced by LPS. Both mechanisms will result in increased PDCD4 abundance, thereby reducing the amounts of the anti-inflammatory cytokine IL-10. The proposed axis for decorin-driven proinflammatory signaling is shown in red.